ABSTRACT

Title of Document: DESIGN AND EVALUATION OF A THERMALLY RESPONSIVE FIREFIGHTER TURNOUT COAT

David Anthony Yates, Master of Science, 2012

Directed By: Professor Marino di Marzo
Department of Fire Protection Engineering

Firefighters, by the intrinsic nature of their occupation, are subjected to a barrage of intense radiant and convective heat fluxes, protected merely by a thin composite layer of fabric for thermal insulation. The exertion requisite of firefighting can raise the temperature inside their turnout coat as well, contributing to the possibility of debilitating heat-related injuries. To mitigate the severity and frequency of such injuries without encumbering the firefighter with excess weight, an assembly of shape memory material was designed that would activate under thermal load to create an insulating air gap between insulating layers in the turnout coat. A prototype gear was constructed and tested, and the heat transfer within it modeled. The enhanced coat was demonstrated to yield a significant performance benefit over a turnout coat without the expanding assembly.

DESIGN AND EVALUATION OF A THERMALLY RESPONSIVE FIREFIGHTER TURNOUT COAT

By

David Anthony Yates

Thesis Submitted to the Faculty of the Graduate School of the
University of Maryland, College Park, in partial fulfillment
of the requirements for the degree of
Master of Science
2012

Advisory Committee:
Professor Marino di Marzo, Chair
Professor Amr Baz
Professor Stanislav Stoliarov

Acknowledgments

I would like to extend my sincerest gratitude to my advisor, Dr. Marino diMarzo, for his unyielding patience and wisdom, candor and insight during the turbulent journey of writing this thesis;

To Drs. Stoliarov and Baz, my thesis committee, for their mentorship and guidance in understanding the principles and practices associated with this project, and with fires in general;

To Drs. Milke and Sunderland, for teaching me the elemental foundations of fire protection as I would come to know them, and for instruction on the art of crafting a technical paper;

To Pat Baker, Sharon Hodgson, and the rest of the miracle workers in the Department of Fire Protection Engineering, for their constant support, understanding, and helpful intercession;

To Justin Perry, Bryant Hendrickson, and James White, for laying the foundation of the work that would go into developing this turnout coat;

To Jason Smoker, Mostafa Nouh, Mohamad Rafat, and James White (again) from UMD, as well as the staff at MFRI including Marty Lepore, for making these test sequences smooth, effective, and even fun;

To Don Aldridge and Lion Apparel for making this research possible, both financially and logistically, and for their faith in the process;

To my housemates, Mitchelle Harris, Maura Donovan, and Xenia Strunnikova, for their understanding, support, and care;

And, most importantly, to my beloved family:

Mom, for teaching me to love.
Dad, for teaching me to live.
Matt, for teaching me to rock.

Without you all, this would not have been possible. A thousand thanks to each of you.

Namasté.

Table of Contents

List of Figures

1. Introduction

This investigation was motivated by a desire to mitigate burn injuries to firefighters in high heat flux conditions. In enclosures with a flaming fire or smoke layer, firefighters can encounter elevated temperatures with intense thermal radiation, causing a dangerous rise in the temperature inside their turnout coat. This temperature rise tends to occur gradually and as the result of a cumulative thermal insult, so a thermally responsive insulation would reduce the rate of and peak temperature rise in the gear.

In addition, an indication to the wearer of a turnout coat that the temperature inside the coat is approaching dangerous levels would provide valuable information in enclosure fires. Many of the thermal injuries sustained by the wearers of turnout gear occur after they have left the exposure, as the hot insulating material continues to conduct heat to the inside. Compression burns, in particular, can occur as firefighters bend their limbs, so delaying the buildup of heat inside the coat with superior insulation is of paramount importance to avoid dangerous conditions continuing after the cessation of exposure.

1.1 Problem Statement

Firefighter turnout coats are a thin layer of protection from intense, unpredictable conditions facing those women and men tasked with the suppression and containment of uncontrolled enclosure fires. The balance between a coat that is heavy enough to provide necessary insulation, yet light enough to permit necessary mobility; a coat that stays dry, but remains breathable from the inside, can mean the difference between safety and burn injury or exhaustion. The best coats, therefore, would contain material of a low density that also effectively insulates against thermal insult.

A turnout coat is desired with thermally responsive properties that would allow it to respond to elevated temperatures, better insulating its wearer and providing him or her with a passive warning about the severity of the fire. This material must too be breathable, to maintain the integrity of the moisture protection afforded by an unaltered coat and in accordance with Chapter 7 of NFPA 1971 [6]. This coat would need to be autonomous in its management of the additional insulation. Although the insulating layer should be effective, it must avoid encumbering the firefighter with a coat that restricts mobility. Finally, this desired material must be cost-effective and able to be implemented with minimal alteration to an existing turnout coat.

A material fitting the criteria for an efficient and effective insulator is air. This investigation examines the design, implementation, and testing of a thermally responsive assembly that opens an air gap inside firefighter turnout gear to afford its wearer extra protection against thermal insult.

2. Literature Review

2.1 Turnout Gear History

As the complexity of fire hazards has increased through history, with it has the protection afforded by firefighter turnout gear. The earliest firefighters in the Americas wore no protective equipment, and structures would routinely burn to the ground because the interior of the buildings would be inaccessible. The 1730s saw the use of the first fire helmet in New York City, but it was not until 1836 that the modern fire helmet was developed by Henry Gratacap for NYFD [1]. Gratacap also suggested the use of wool as a thermally insulating material to protect firefighters from heat, with an additional cotton or wool undershirt. [2,3] Rubber boots and long trench coats were utilized to provide moisture protection, as well as mitigating the degradation of thermal protection wrought by water saturation of insulating material [2] 1863 saw the first SCBA gear implemented by James Braidwood, using rubber-lined canvas bags to provide air to firefighters inside smoky buildings.

The modern firefighter turnout coat was developed after World War II, as the NFPA prescribed standards for requisite thermal protection of firefighter safety gear. These standards became NFPA 1971-1986 [4], and provided the basis for the composite firefighter gear in common use today. A three-layer garment was used, with a flame resistant outer layer, an intermediate moisture barrier, and a thermally insulating inner layer [4], forming the basis for the garment studied in this study. Different configurations of outer shells were used to provide specific protection against chemical or radiological hazards, and Lion Apparel developed several lines of clothing in search of an ergonomic balance between thermal protection and unrestricted mobility [5]. The NFPA revised the minimum required level of thermal protection in the 1980s to a 1200 F resistance rating, as well as requiring sensors to indicate if a firefighter has stopped moving [4,6]. The standard continues to see revisions, even today, to better protect firefighters from dangerous conditions.

2.2 Heat Transfer Studies

There have been numerous investigations quantifying the thermal protective performance of firefighter safety gear, using both experimental measurements and numerical models. Attempts to reconcile the two have, with some success, described the heat transfer processes inside firefighter gear, but work remains to be done in the characterization of the thermal properties of the coat. NFPA 1971 laments a disconnect between the testing of gear in a laboratory setting and its actual performance [4], particularly respecting the working environment in which the turnout coat can be relied upon to deliver a stated level of insulation, but others [7] have shown that, qualitatively, the relative performance of gear in a laboratory setting is a good predictor of its actual performance. Torvi [7,8] was able to mathematically describe the influence of air gaps on the thermally insulating properties of turnout gear, as well as some of the fabric thermal properties for different test conditions. He cited a value for the emissivity of the fabric around 0.9, as well as a nominal convective heat transfer to the fabric of 40 kW/m^2, in bench-scale testing. He also, interestingly, described the entire sample as being heated uniformly on its surface. Although the same is obviously not true in actual firefighter turnout gear, the length scale across the coat is so much smaller than the associated conductive length scales parallel to the surface of the coat that the assumption of one-dimensional conduction in an actual coat is a reasonable one at any given point on its surface; that is, lateral effects of heating can be neglected pointwise in bench-scale testing. It is important to note that this does not mean that the interior of the gear will be heated uniformly; for example, the top of the gear will receive radiant heat from the upper layer that the underside of the arms would not. The geometry of the air gap enclosing adjacent layers of the coat, however, is not so simple; although an effective thermal conductivity is used to describe both the radiation and convection heat transfer, the fit of the gear affects the width of the air gap and, thus, its protective performance. The bench-scale test specimens were mounted horizontally, but would have a different configuration when actually worn. The weight and tension of the fabric, therefore, could compress the air gap in a way that was not modeled in the bench scale.

Torvi [9] also described the thermal processes leading to second degree burns through insulating material by way of the Stoll curve [10], the critical conditions leading to burns in different layers of skin under different heat fluxes. The criterion described a critical heat flux for a given time that would lead to second-degree burns, with the intuitive finding that higher heat fluxes would cause burns in shorter periods of time. The critical heat fluxes are presented in figure 2.1. Stoll also related the heat fluxes to rates of temperature rise of a copper calorimeter to facilitate laboratory measurement.

Exposure Time (s)	Heat Flux (kW/m^2)	Total Heat (kJ/m^2)
1	50	50
2	31	61
3	23	69
4	19	75
5	16	80
6	14	85
7	13	88
8	12	92
9	11	95
10	9.8	98
11	9.2	101
12	8.6	103
13	8.1	106
14	7.7	108
15	7.4	111
16	7.0	113
17	6.7	114
18	6.4	116
19	6.2	118
20	6.0	120
25	5.1	128
30	4.5	134

Figure 2.1: Stoll critical burn heat fluxes.

Zhu, et al. [11] also characterized the thermal insult to skin in a cylindrical geometry to describe the shape of the arm or leg. In these cases, the investigated parameter was the delay between cessation of heating of the turnout coat and subsequent cessation of heating of the skin, called a “thermal relaxation time”. This characterized the length of time the inside of a turnout coat would continue to transfer heat even after the exposure to the outside was removed.

2.3 Moisture Transport Studies

The degradation of performance of firefighter safety gear due to moisture is of significant concern due to the profuse sweating of firefighters during fire conditions, as well as water vapor from fire-fighting activities. The amount of moisture in a given fabric is presently defined by the regain, the ratio of the weight of water in a material to its dry weight.

$$regain = \frac{m_{water}}{m_{fabric}}$$

Liquid phase moisture in fabric has, interestingly, two conflicting effects on heat transfer: it increases the thermal conductivity of the fabric, but also increases the specific heat and density. This is important because the temperature rise in the gear is governed by the thermal diffusivity, with the thermal conductivity in its numerator and the specific heat and material density in the denominator. The stitch pattern and density of the fabric are related: a higher stitch density will yield a fabric with a higher material density, but both have a lower effect on the thermal conductivity than the moisture content or thickness, which instead vary strongly with both regain and porosity [11]. Less porous fabrics had more rapid increases in thermal conductivities with regain, likely owing to their higher fabric (and therefore mass) density. Diak, et al. [12] encountered difficulties measuring the temperature between two fabric surfaces, due to the pointwise nature of thermocouple temperature measurements. Instead, such a temperature gradient is more readily measured using a device that analyzes the net heat flow through the fabric. Pointwise temperature measurements are susceptible to variation in lateral distribution of moisture and, consequently, non-uniform heat flow through the cross-section. In this research, the pointwise temperature was assumed to be indicative of the overall conditions inside the turnout coat, and the thermal properties of the investigated medium were assumed uniform in an effort to assess the performance of the turnout coat.

Moisture saturation, especially in high heat flux conditions, has the competing effect of providing some insulation against thermal insult. Water outside the moisture barrier in firefighter turnout gear, from external sources such as hose sprays, increases both the thermal conductivity and the heat capacity; these competing effects at different levels of regain have yet to be investigated [13]. Inside the moisture barrier, the effects of moisture are generally deleterious; in addition to degrading the thermal insulation of the inner layer, moisture inside also has potential to condense on the skin, causing steam burns. One simplifying model assumption employed by Perry [14] is that moisture that enters the vapor phase inside of the moisture barrier immediately exits the assembly, either through the legs or the arms, and does not condense on the surface of the skin. The validity of this assumption should be examined, with careful attention to the moisture / skin interface and its effects on the heat flux to the surface. In addition to the thermal insult, the heat flux due to vapor condensation could contribute to the Stoll burn criterion previously described in table 2.1.

Perry [14] refined a numerical model developed by Spangler [29] to characterize the effects of moisture on the performance of an insulating layer of turnout gear. Using a Crank-Nicolson scheme and known thermal properties of the different layers, he successfully matched model results to known curves capturing moisture-affected thermal properties, validating his work with a closed-form solution and corroborating the results with experiments [17] based on test standards [18-20] that offer a systematic way to determine the thermal protection afforded by a given type of insulation. Perry modeled the changes in thermal conductivity that accompany different regains, lending credence to the work done by Schneider [21] that described these same changes. Qualitatively, the thermal conductivity is a definitive function of regain. Perry curve-fit this effect using a two-part linear rate of increase in thermal conductivity with regain, increasing steeply for regain below 0.2 and more slowly for regain above 0.2. This effect is displayed in figure 2.2.

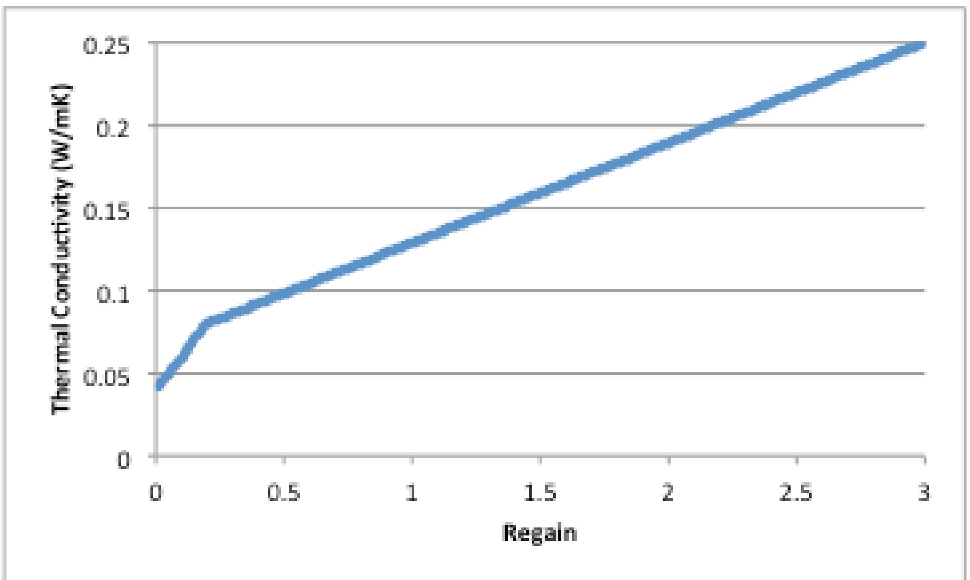

Figure 2.2: cotton thermal conductivity as a function of regain [14].

2.4 Air Gap Studies

Hendrickson [15] described the changing temperature as a function of space and time of a composite material with an air gap that varied in size. This investigation was critical for understanding the effect of a thermally responsive material, but posed a unique challenge; when modeling an expanding layer in a one-dimensional simulation, the spatial domain changes size, and the simulation must accommodate this. Rather cleverly, he introduced a parameter that subsumed the ratio of the height of the air gap to the initial height, collapsing the time dependency of the variable air gap height into a single parameter that can effect changes on the system as a whole. In addition, his approach considers both radiation and convection inside the air gap layer, increasing the fidelity of the simulation to real test conditions.

White [17] contributed validation data to the work of Perry and Hendrickson, using a moisture plate and a fixed air gap to capture both effects evaluated by his predecessors. These experiments would serve as the calibration for the comprehensive numerical model employed in the present study. Using a long (~10 minute) uniform exposure to a radiant heater, White heated swatches of samples obtained from Lion Apparel from the different insulating materials of the turnout coats they supply. By placing thermocouples between each of the layers of sampled turnout coat, White was able to characterize the steady-state temperature gradient across the turnout gear. These normalized temperatures profiles would serve as calibration data for the model developed in the present investigation. White used a moisture plate to emulate perspiration of firefighters in actual test conditions. White also described the behavior of a thermally responsive air gap using the shape memory material described in [15]. In addition, he varied the configuration for the layers of insulating material, and was therefore able to optimize a configuration of gear that performed markedly better without adding much bulk to the gear.

3. Gear Design

The addition to the firefighter turnout coat employed in this investigation depended on the use of a phase-changing nickel-titanium alloy to stiffen into a rigid form, creating an air pocket on the arms and shoulders of a firefighter turnout coat. Practical design constraints were considered, including the limitations associated with a bulky or heavy coat, as well as the ease with which the air pocket could be generated. The configuration with the greatest potential to mitigate burn severity was, therefore, desired in this project.

Hendrickson and White [15,17] developed a mathematical model for and experimentally validated the insulating performance of a firefighter coat assembly that utilized shape memory material (SMM) to create an air gap between insulating layers. This shape memory material will be described, and its implementation evaluated. Later, a mathematical approach for modeling the expansion of the air gap will be developed based on the work done by [15].

3.1 Shape Memory Material Background

A nickel-titanium alloy fashioned into wire loops was used by Baz [15], and through repeated heating and quenching, the material was “trained” to change phase at a prescribed temperature, a phase change that would define a new set of material properties. Below the activation temperature, the material is malleable in the martensite phase, but as it heats, the phase change occurs and the material becomes rigid in the shape to which it was trained as austenite.

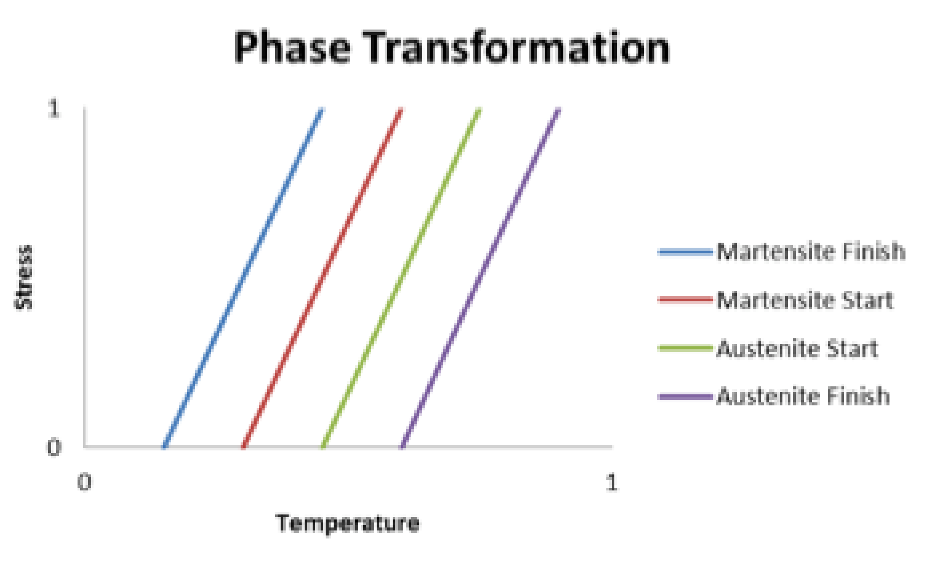

Figure 3.1 Phase transformation of shape memory material [15].

Research by Tanaka [18] shows that the stress-temperature lines corresponding to the phase changes are parallel. A material undergoing an increase in temperature starts initially in total martensite (a malleable form), increasing to incipient transformation to austenite at the temperature-stress coordinate demarcated by "austenite start" until such time as it reaches a steady state of total austenite. The process is reversed in the other direction. The transformation can occur under physical stress as well, but was not investigated in this study.

In this implementation, one wire of shape memory material was fashioned into two conjoined loops held in the center by a clip, forming a butterfly shape. In the martensite phase, the loops would remain malleable and could be laid flat, but when heated, would stiffen such that the center of the assembly rose above the ends. The activation temperature of the SMM rings used in this implementation was 50 C. Figures 3.2 show pictures of the butterflies in each phase.

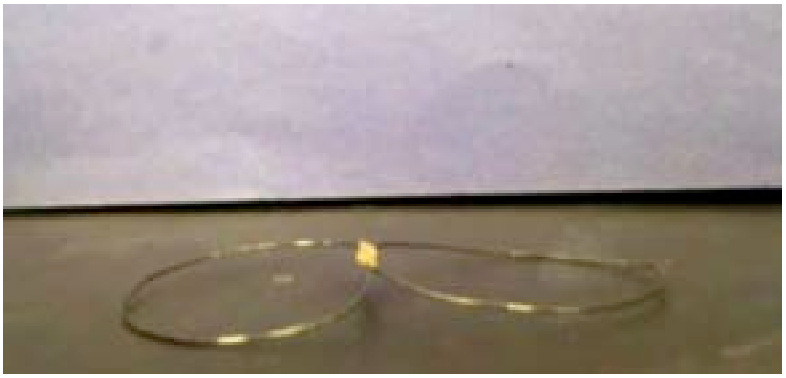

(a)

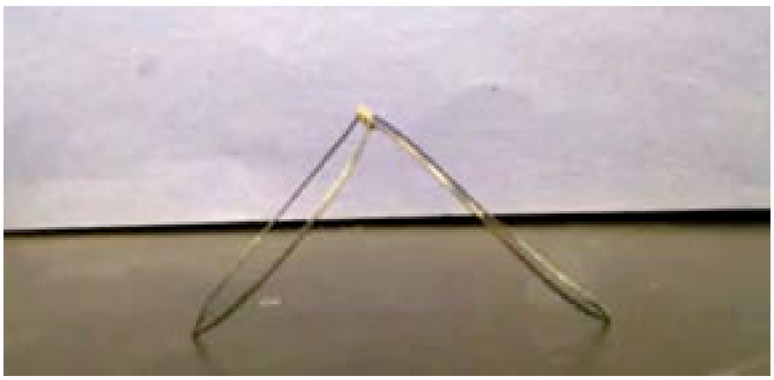

(b)

Figure 3.2: shape memory butterflies in martensite (a) and austenite (b) configurations. Pictures courtesy of Hendrickson[15].

3.2 Existing Turnout Gear

The turnout coat utilized in the present investigation is a composite material developed for use by Lion Apparel [5] and with a layer configuration modified in an investigation by White [17]. This coat is a composite material comprised of a thermal liner, moisture barrier, face cloth insulating layer, and outer shell material, a design based on the C-liner marketed by Lion Apparel. Each component of the coat serves a unique purpose in protecting its wearer from thermal insult and moisture saturation. The Glide and E89715M thermal liners utilized presently provide insulation against thermal insult, and the former some degree of moisture protection at the inner face of the coat. The Crosstech moisture barrier prevents moisture from penetrating the coat in either direction, from perspiration on the inside or from fire spray or other sources outside. A Chambray facecloth layer outside of the moisture barrier provides additional thermal insulation. In this investigation, this facecloth was doubled to include pockets where the shape memory rings would enclose an air gap. The PBI matrix outer shell completes the turnout coat assembly, protecting against direct flame impingement. The specific details of the implementation of the shape memory material in the turnout coat will be outlined in the next section, but figure 3.3 shows the arrangement of the layers of material that are presently employed. Properties of each of the material layers are tabulated in appendix C.

<table>
<tr><td>PBI Matrix</td><td>Outer Shell</td></tr>
<tr><td>Chambray</td><td rowspan="3">Shape Memory Material Assembly</td></tr>
<tr><td>SMM</td></tr>
<tr><td>Chambray</td></tr>
<tr><td>Crosstech</td><td>Moisture Barrier</td></tr>
<tr><td>E89 715M</td><td rowspan="2">Thermal Liner</td></tr>
<tr><td>Glide</td></tr>
</table>

Figure 3.3: Layers of composite turnout coat with shape memory material included.

3.3: Implementation In Present Investigation

The effectiveness of reinforcing the firefighter turnout coat using the shape memory rings depended on the capacity of the turnout coat to expand and open an air gap. This functionality required unrestricted movement of the coat normal to the layering of material, so heavy objects that restricted the capacity of the air gap to open limited the opportunities for useful placement of the shape memory material. In addition, most of the thermal insult to the turnout coat is driven by radiant heat from hot air, enclosure surfaces, and fire, so the most effective placement for the shape memory material was one that allowed them to insulate against heat flux from these sources.

The shape memory rings were placed in the external Chambray insulating layer. Stitching pockets between layers of facecloth made for an assembly that was easy to manufacture and relatively lightweight in comparison to the other layers of material present in the assembly. In addition to providing additional insulation, placing the rings close to the outside of the turnout coat allowed them to activate quickly in response to an external heat flux. In so doing, they change phase before the thermal insult has penetrated the turnout coat, providing the maximum possible insulation that they can offer.

In addition to the placement within the layers of the turnout coat, the location of the shape memory rings on the turnout coat was an important design consideration. In fire conditions, most of the heat flux to the turnout coat comes from radiant heat, from a flame source and from a hot upper layer. Therefore, it is the exposed areas on the coat that are most in need of protection, including the arms and shoulders, chest and back. (Protecting the firefighters' head and legs was beyond the scope of this investigation.) Firefighters in full turnout gear carry a heavy oxygen tank on their back that would restrict expansion of the back of their turnout coat, and the straps to secure this tank are taut on the front of their coat. The most useful location of the shape memory material, therefore, is on the outside of the arms and shoulders of the turnout coat, where it would be exposed to radiant heat from the hot upper layer and from a flaming fire, and where the shape memory material would be able to effectively expand.

The insulating facecloth layers were stitched together in a way that created pockets for the butterflies, with adjacent butterflies inverted with respect to one another. By having adjacent butterflies inverted, a symmetrical and level expansion of the entire assembly was achievable. A schematic of the SMM assembly and pocket configuration is depicted in figure 3.4.

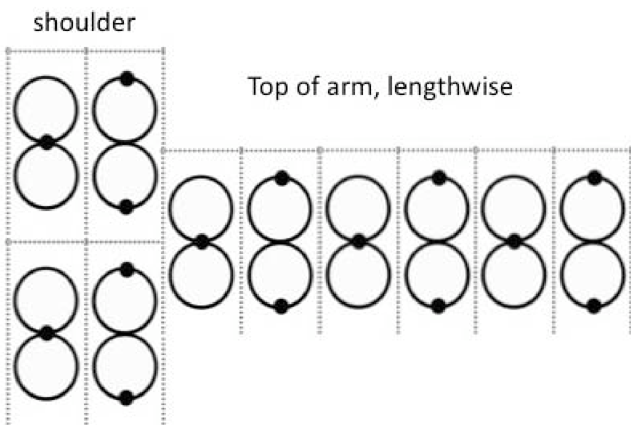

Figure 3.4: shape memory pocket configuration.

The dark circles demarcate high points of the expanded rings; a circle on the inside indicate a ring that expands in the configuration shown in figure 3.2(b), while circles on the outside indicate an inverted butterfly with high points at the edge of its wings.

By stitching each pocket individually, the rings could be taken out and different configurations tried. In this investigation, a double ring assembly was also tried with two butterflies in the same configuration placed into pockets to assess whether one ring stiffening by itself would have sufficient physical strength to open a large enough air gap to provide significant protection.

Figure 3.5 shows the double facecloth layer as implemented in the shoulder pocket of the turnout coat, with the ring assembly peeking from the pocket.

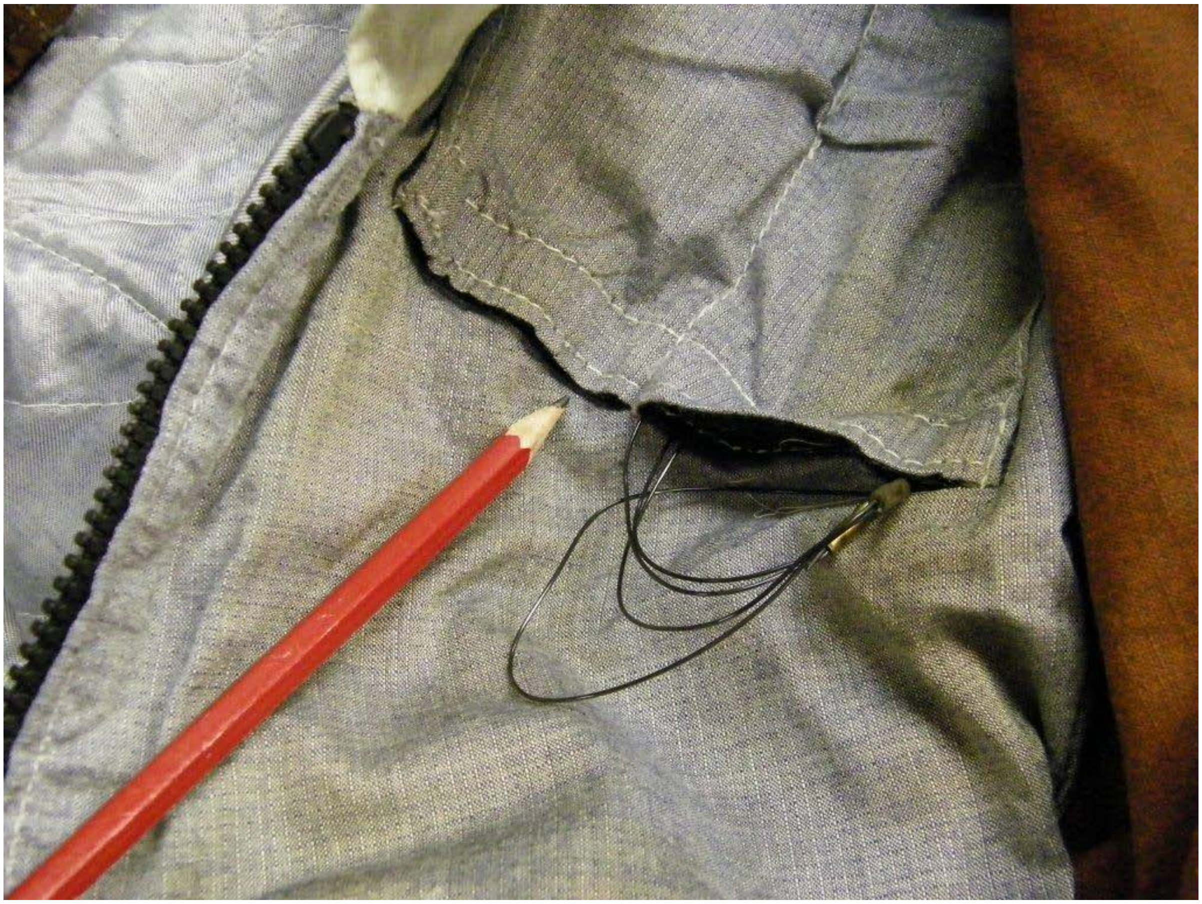

Figure 3.5: Shape memory ring as implemented

4. Experimental Methods

The present investigation is concerned with the improvement of firefighter turnout coat wrought by the inclusion of a shape memory material in the coat design. Previous investigations [15,17] have demonstrated the benefit of including the shape memory material or air gaps in a general sense in a laboratory setting. Bench-scale tests, however, are not sufficient to draw conclusions about the efficacy of the coat in practice, so a test was devised for the evaluation of the value of the expanding coat by comparing it head-to-head with a regular turnout coat.

In an effort to understand the changes in performance relevant to this investigation of firefighter safety coat, it is necessary to first identify the different criteria by which the comparative performance will be assessed. The crux of this study is the comparative performance of the regular and enhanced coat, the change in performance wrought by the inclusion of the shape memory material. Only the change in one portion of the coat, the outsides of the shoulders, will be measured directly. The performance of the expanding coat was investigated for its effectiveness over a wider range of conditions. Some tests were performed with two SMM rings instead of one; this was characterized for its performance benefit. In addition, data were assessed based on the number of tests that had been conducted that day, to ascertain possible effects of stored heat in the walls of the room.

4.1 Room Layout

The full-scale tests of the thermally responsive gear were conducted at the Maryland Fire and Rescue Institute (MFRI) in College Park, Maryland, in two series of a ten days each: from 28 November to 9 December 2011, and 26 March to 6 April 2012. Tests were conducted on the third floor of the burn building, with supervisory assistance on the second floor of the same.

Figure 4.1 depicts a schematic of the burn room.

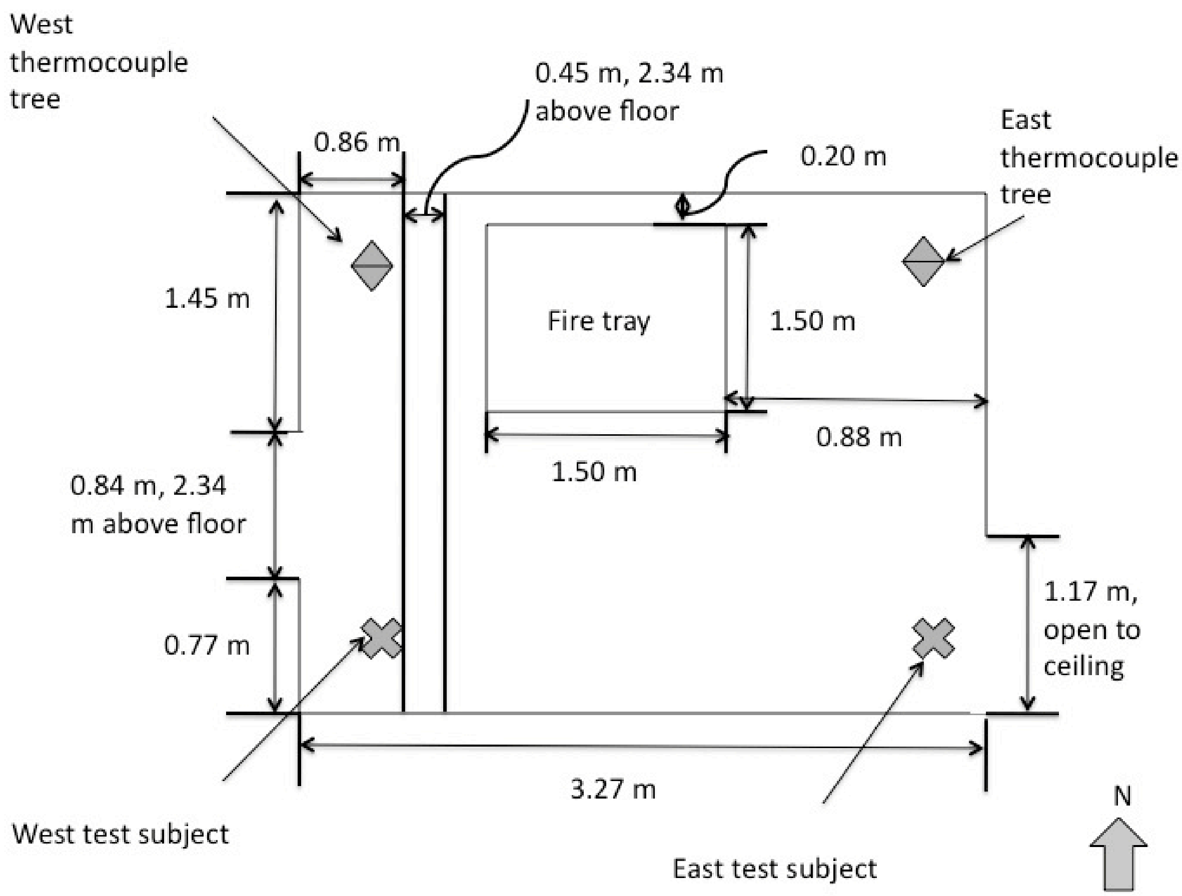

Figure 4.1: Test enclosure schematic.

The test enclosure is a concrete room with cinder block walls, about 3.1x3.3x2.8 m, with openings at either side. The openings into the room are asymmetrical: the west opening is 0.8 m wide and 2.0 m high, and the east 1.2 wide and open up to the ceiling. A beam extends 45 cm down from the ceiling, 45 cm wide, located 86 cm from the west wall. The room is empty, but for these obstructions. A raised 1.5x1.5 m tray is located 20 cm from the north wall in the center of the room, upon which wood pallets and shavings are placed for burning.

The rooms adjacent to the burn room are different sizes. The adjacent room through the east door is significantly smaller than the west. This discrepancy in size affected the air currents in the room and stratified the location at which the smoke layer formed; the pressure differential associated with a wider open space outside the west door resulted in a higher neutral plane at the location of that door than at the east. The effects of this stratification will be examined after the fire is described.

Fig. 4.2: Test enclosure through west door facing east.

The fire tray was loaded with three wood pallets, in a triangle shape surrounding ¼ of a nominally 77-lb bale of wood shavings. The fire was ignited from the wood shavings using a flare.

Fig. 4.3: Wood pallet arrangement and ignition.

This exposure was highly variable within and between tests; some fires would be more severe than others, and burn for shorter or longer durations or require additional stoking. During each test, a total of one-quarter of a bale of Excelsor wood shavings was added to the pallet pyramid through the duration of the test. Depending on the relative severity of the fire, the firefighter adding the shavings to the fire would sometimes wait until partway through the test to stoke the fire or to pile on additional shavings. In some tests, different wood pallets were used, and in later tests, as the weather grew warmer and the walls stored more heat, two pallets were used instead of three, stacked atop one another with the shavings in between. The intrinsic chaos of a full-scale fire is well-known, and these fires were no exception; because of this, they helped to provide a wide cross-section of different exposures to the coats.

Although a pre-burn was performed most mornings to raise the temperature of the room, the cinder block walls were slow to dissipate heat throughout the day, and the later tests tended to be more intense and hot than earlier ones. Also worth note is that the morning and afternoon tests were separated by a lunch break of about an hour; the burn room cooled some during this time, but not nearly as much as it did overnight.

4.2 Instrumentation

4.2.1 Temperature Buttons

The temperature buttons on the sides of the firefighters' shoulders collected data from the interior of the turnout coat that was used to assess their performance. These buttons were placed into pockets sewn into the left and right sides of the cotton shirts worn by the test subjects, depicted in figure 4.4. The east side firefighter wore buttons "A" and "B" on his left and right shoulder, respectively, and the west side "C" and "D" on the same shoulders.

Figure 4.4: Location of temperature button on firefighter's shoulder.

The temperature buttons utilized in this experiment were selected based on the preference of Lion Apparel, but were prone to drift in the recorded temperature and time that limited their reliability in both respects. The temporal drift caused a disconnect between the measured time recorded by the buttons and the clock time, making it impractical to identify the precise start time of each of the experiments. In addition, the temperature drift created uncertainty in the total temperature rise inside the coat, so although the readings were self-consistent, the absolute temperature values recorded by the buttons could not be compared. In order to minimize the effects of the drift in each of these cases, the rate of temperature rise was investigated.

The button temperatures were collected every two seconds. Each of these values was plotted, and the rate of temperature rise was found by a visual linear fit of the data in Microsoft Excel. This fit captured the steepest slope of the button temperature rise for each test; to find the rate of internal temperature rise, this slope was divided by two. The collected fits for all of the buttons in the spring test series are visible in appendix A. An example fit is shown:

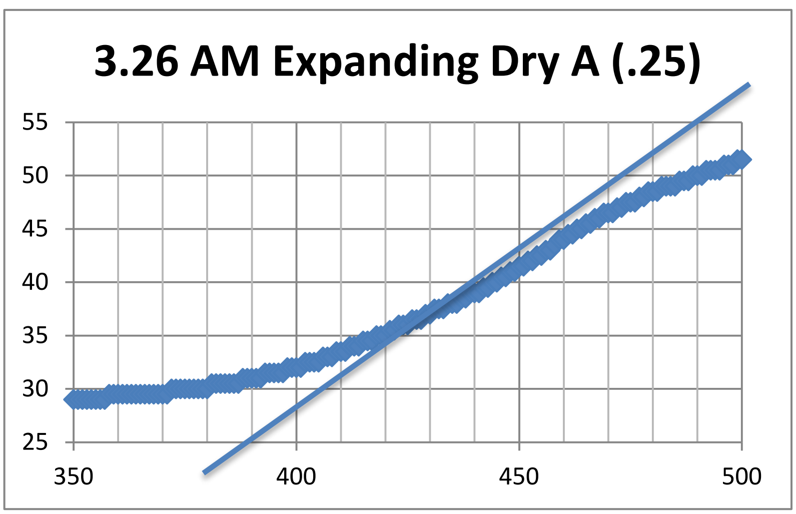

Figure 4.5: linear fit for button A temperature data from the first test of 3.26; a slope of 0.25 gives a rate of temperature rise of 0.13 C/s.

4.2.2 Thermocouple Trees

Thermocouple trees were placed 40 cm from the east and west walls, about 1 m south of the north wall. Six thermocouples were attached to each of the trees. The heights are 2.4, 2.0, 1.5, 1.1, 0.6, and 0.15 m from the floor. On the schematic drawing in 4.1, the thermocouple trees are depicted as grey diamonds.

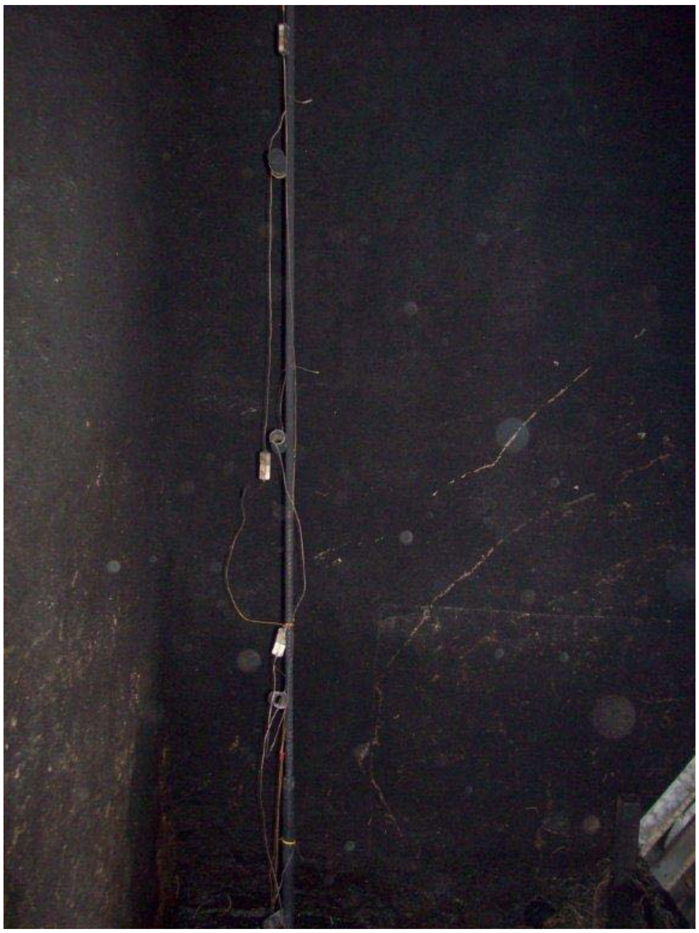

Fig. 4.6: Thermocouple tree.

The temperature stratification in the room was captured by a thermocouple tree oriented next to the fire. As an example, the temperature with height through time for the first test on 28 Nov. 2011:

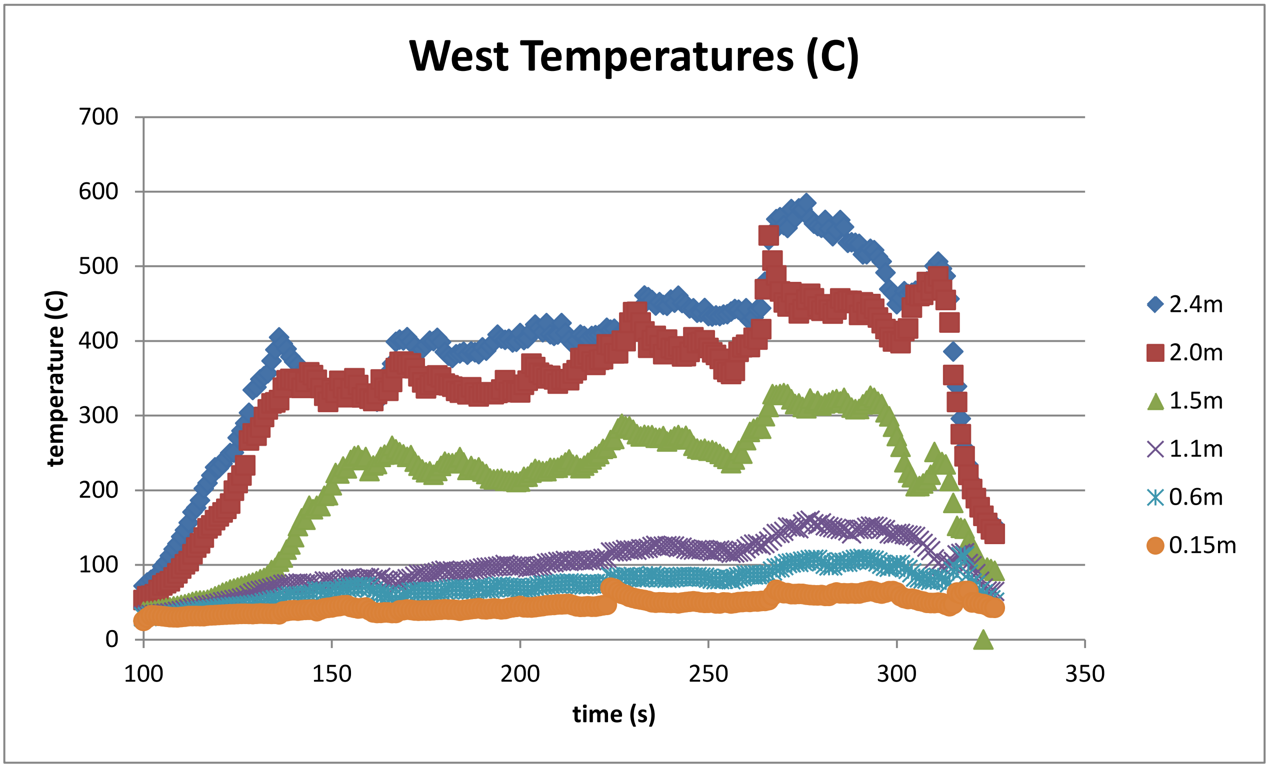

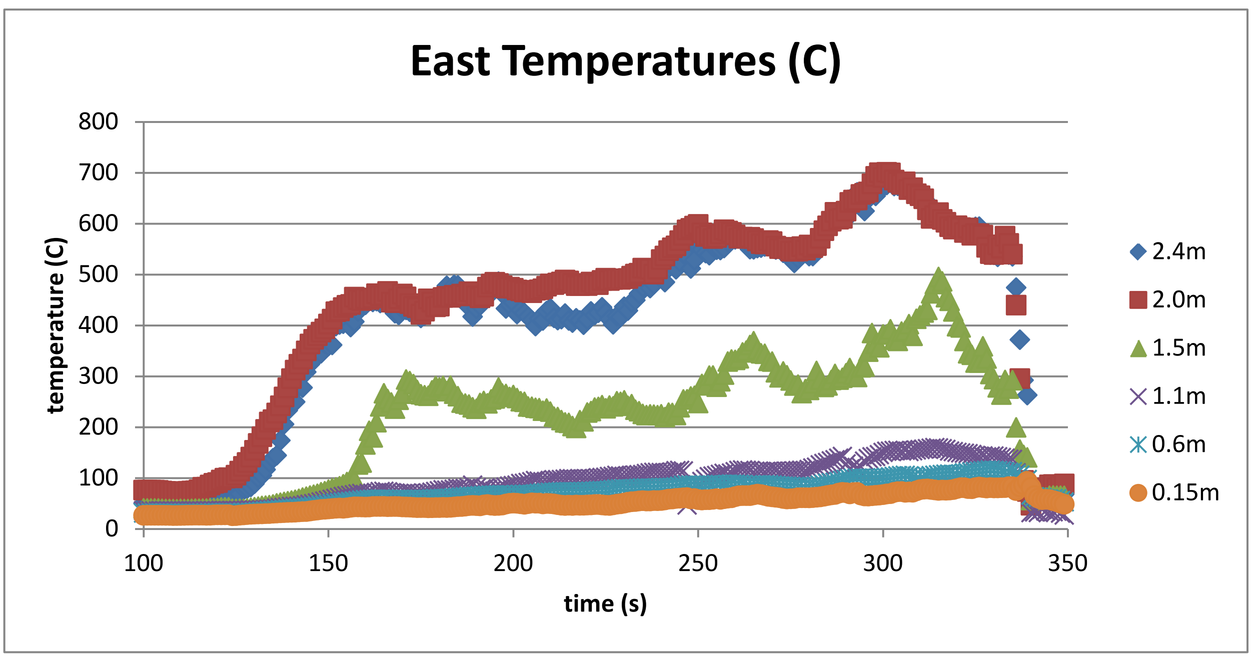

Figure 4.7: Thermocouple readings for first test on 28 November.

Average temperatures on the east side of the room were consistently higher than the west side, sometimes by as much as 200 C. These temperatures were measured next to the fire, however, and not next to the firefighters; thus, the exposure temperature of the coats can not be matched directly to the thermocouple reading.

Figure 4.2 depicts the incipient stages of a fire as it slowly begins to engulf the enclosure. A visible smoke layer is beginning to form, but the firefighter in the picture is able to stand erect in the room. The smoke layer in the room formed fairly consistently in the same location, as evidenced by the stratification in figure 4.7, between 1.1-1.6 m from the floor.

The thermocouples' reported values were subject to some divergence from the conditions in the room experienced by the firefighters' turnout coats. The effects of thermal radiation on thermocouple readings is unknown and may have affected the reported temperatures. The magnitude of absorbed radiation and re-radiation from the thermocouples was unknown, and further confounded by the deposition of soot on the thermocouple leads over the course of several fires. In addition to the different radiative properties of the thermocouples with respect to the firefighter gear, the location of the thermocouples in the room was not representative of the conditions on the outside of the coats. The firefighters were located closer to the door than the thermocouples, so the air temperature was affected by the transport of hot air and smoke from the room. In addition, the thermocouples were closer to and more directly facing the fire than the firefighters' temperature buttons, which were on the outside of the shoulders, while the firefighters themselves faced the fire.. As a consequence, they were likely to receive a much higher radiative heat flux than the firefighters, making them unhelpful for recording exposure temperatures on the coats. Their readings are still helpful for understanding conditions in the room, respecting the location of the smoke layer and temperature stratification across the room.

4.3 Test Subjects and Matrix

Two firefighters served as test subjects in each experiment; in total, four firefighters were test subjects, and pairs would alternate days of testing. Both test subjects wore full turnout gear, complete with SCBA and helmet, boots, insulated pants, and gloves, as did all of the other supervisory personnel on the burn floor. Not less than three additional firefighters were on the burn floor during tests. It was observed after the first two days of testing that subjects in the standing position quickly led to a number of facemasks being damaged by the high incident heat fluxes, so test subjects wore a second hood backwards over their facemasks to protect them and provide an additional layer of protection from heat flux to their faces. In addition, for tests on 2 December and later, test subjects were instructed to kneel within the fire zone to reduce their exposure to hot gases. Since the introduction of the second face hood, no facemasks were damaged.

Fig. 4.8: Test subject with extra hood.

The two firefighters stood just inside the east and west doors, facing the fire tray; their approximate location was depicted by the “x” in figure 4.1. They waved their arms low and close to their body to simulate possible motion inside a fire zone and to determine any restrictions on mobility caused by the expanding firefighter coat. On the first test of each day in both series, the firefighter standing at the east door wore the regular turnout coat, and the west door wore the expanding coat (in the first week of testing in the spring, expanding coats with one and two rings were tested in lieu of regular and one-ring expanding, respectively). After the first test in the morning, they switched coats and stayed at the same door, their test position for the duration of the day’s tests. In the afternoon, they wore the same coats as in the second morning test, before switching again for the fourth test. A chart indicating the locations of each of the coats and the test condition is presented for clarity:

Table 4.1: Orientation of Turnout Gear

	AM		**PM**	
Test	**1**	**2**	**3**	**4**
East	Reg	Exp	Exp	Reg
West	Exp	Reg	Reg	Exp

Fires were ignited and allowed to develop before the test subjects entered. When thermocouple readings of 150 C were observed at both trees at the 1.5 m thermocouple, subjects were simultaneously instructed to enter. A staggered entrance was used for the first three days with the intention of discouraging competition between firefighters to see who could stay in the burn room longer. This protocol was subsequently discarded, as it was shown to be unnecessary. In the fall test series, firefighters were instructed to leave when they subjectively began to observe a rapid temperature rise inside their turnout coat, indicating that the exposure heat had penetrated the coat. In the spring series, in an effort to standardize the exposures between days, tests were concluded three minutes after the firefighters entered.

5. Results

Summary statistics are reported below. For each test, the percent difference in rate of temperature rise between the expanding and regular gear was plotted using the following formula:

$$\%diff = \frac{\left.\frac{dT}{dt}\right|_{reg}}{\left.\frac{dT}{dt}\right|_{\exp}} - 1$$

It is worth note that this percent difference is divided by the rate of change for the expanding, rather than the regular test. A more standard convention might be to divide the difference in the rates of temperature rise by the regular, but since the expanding test is likely to yield a shallower rate of temperature rise than the regular, trends highlighting the difference in performance become more evident when the rate is divided by the generally lower rate of temperature rise of the expanding gear.

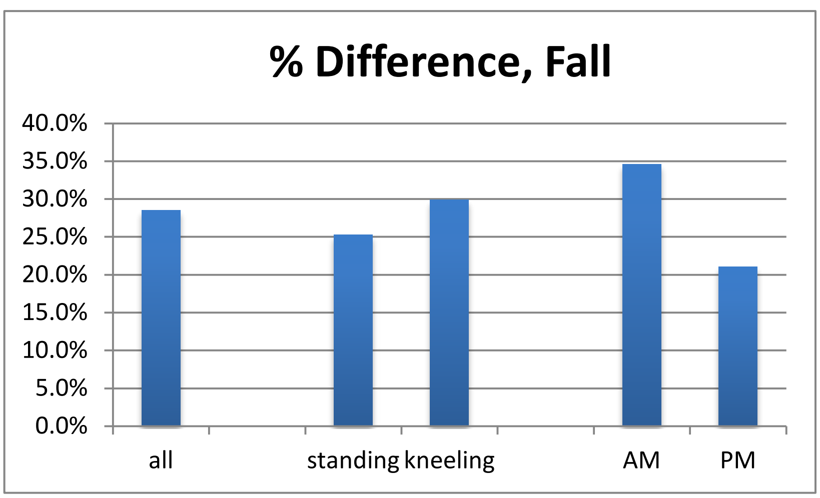

Figure 5.1: Percent difference in temperature rise, fall series

Table 5.1: Statistics for temperature rise, fall series

	n	avg.	median	Q1	Q3
all	40	29%	20%	3%	56%
standing	12	25%	27%	8%	42%
kneeling	28	30%	16%	1%	47%
AM	22	35%	25%	6%	68%
PM	18	21%	20%	-2%	46%

In the fall series, the average percent difference in normalized rate of temperature rise between the coats indicated an average 29% difference between the expanding and regular coats. This effect was most pronounced in kneeling tests and in tests conducted in the AM. The middle 50% of tests reported percent differences between 3 and 56% for all tests; this range was higher for the AM tests than for PM, but narrower and with a smaller range for the standing tests compared to the kneeling.

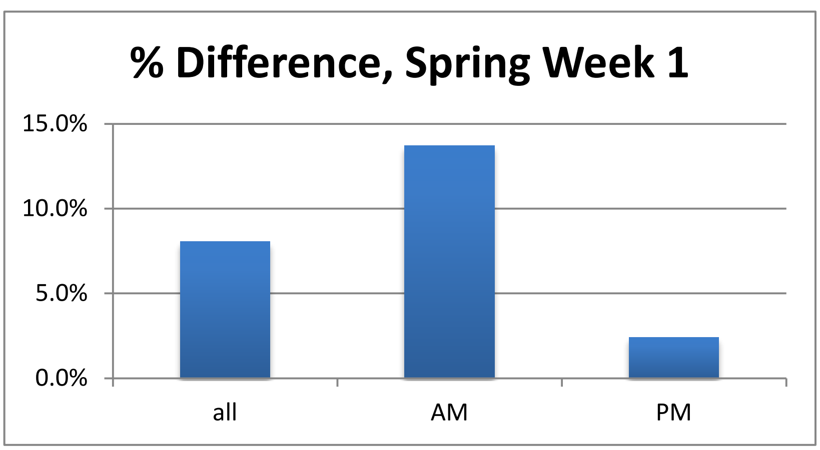

Figure 5.2: Percent difference in temperature rise, spring week 1.

Table 5.2: Statistics for temperature rise, spring week 1.

	n	avg.	median	Q1	Q3
all	20	8%	7%	-18%	18%
AM	10	14%	-2%	-24%	12%
PM	10	2%	13%	2%	16%

The tests in the first week of spring compared the effects of one expanding ring with two to see if the addition of a second would provide extra reinforcement of the expanding air gap. This series demonstrated an 8% difference between two and one expanding ring, with an interquartile range centered at 0%. This does not suggest an improvement in protective performance wrought by the inclusion of a second SMM ring. The average percent difference of the two-ring expanding coat was higher in the morning tests than the afternoon, but the opposite trend was observed in the median; the single test with a very high percent difference in the AM series skewed the average positively, and so the performance benefits of including a second expanding ring are inconclusive.

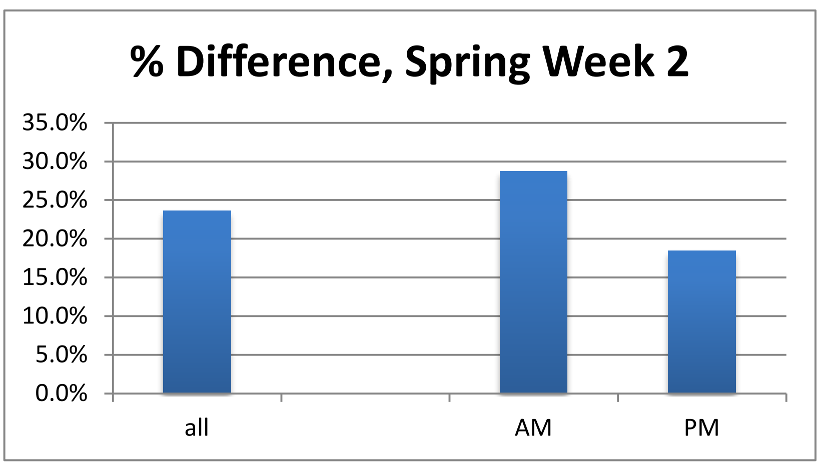

Figure 5.3: Percent difference in rate of temperature rise, spring week 2.

Table 5.3: Statistics for temperature rise, spring week 2.

	n	avg.	median	Q1	Q3
all	20	24%	7%	-22%	70%
AM	10	29%	7%	-32%	72%
PM	10	19%	4%	-19%	54%

The spring week 2 tests showed, on average, a 24% difference between the expanding and regular coats. Again, the average and median percent differences are higher in the morning than afternoon tests. The wider interquartile range present in this test campaign indicates significant fluctuations in the sampled data.

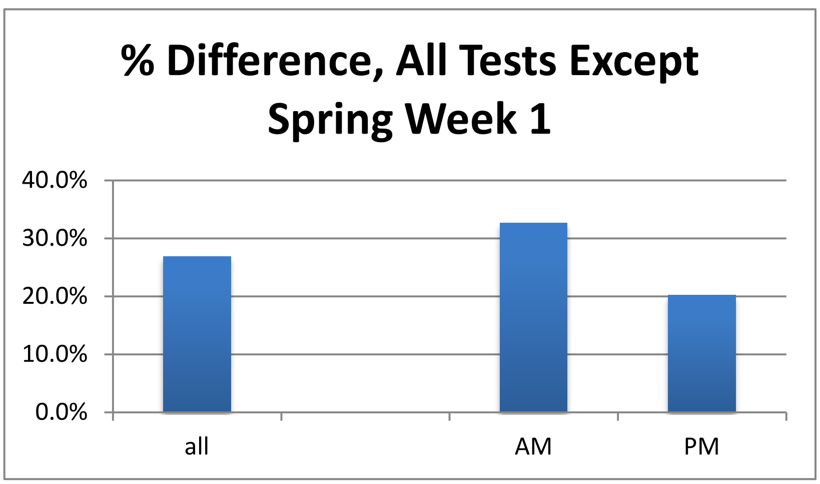

Figure 5.4: Percent difference in rate of temperature rise, all tests except spring week 1.

Table 5.4: Statistics for rate of temperature rise, all tests except spring week 1.

	n	avg.	median	Q1	Q3
all	80	27%	16%	-10%	42%
AM	42	33%	18%	-1%	68%
PM	38	20%	13%	-15%	31%

When all of the tests are collected, omitting the two vs. one ring comparison, an average 27% difference between expanding and regular coats is observed. As before, this trend is most pronounced in the morning tests, with a percent difference of 33%, than compared to the evening tests, with a percent difference of 20%. The medians in each case are lower than the averages, indicating some positive skew; this means that the highest percent differences are further from the mean than the lowest.

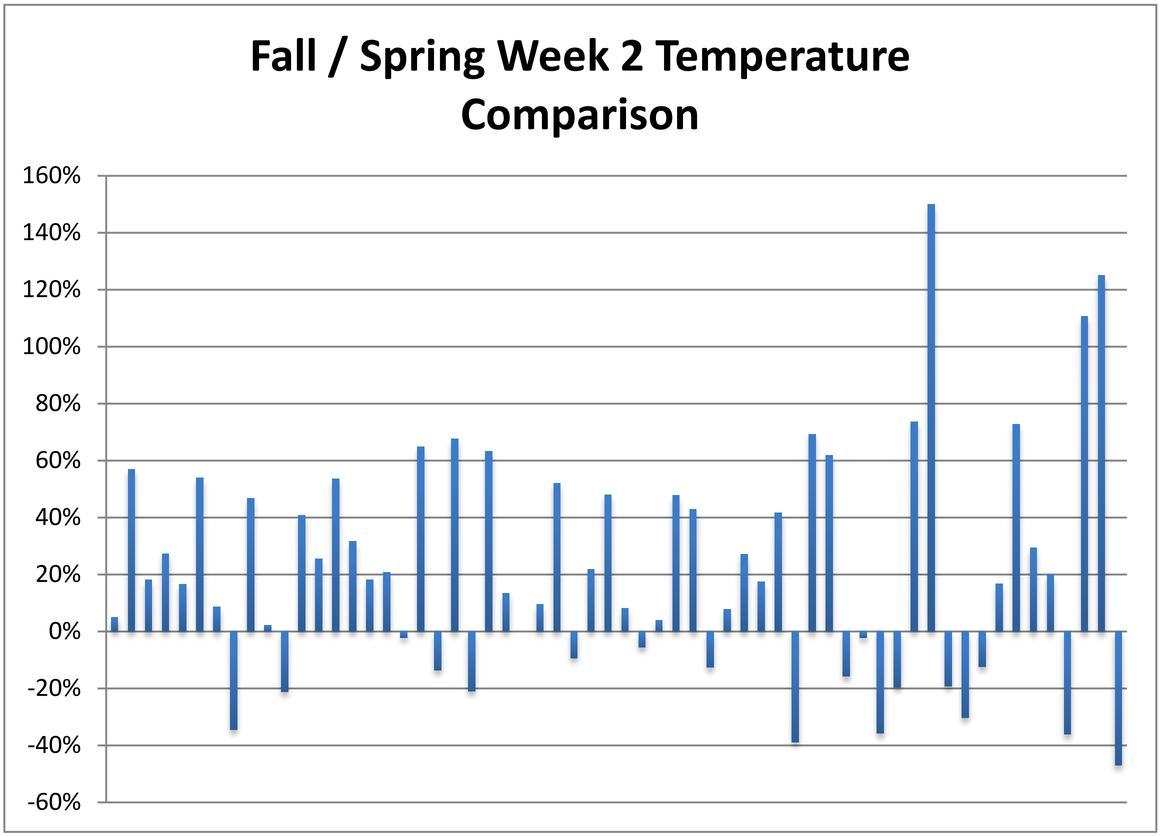

Figure 5.5: Comparison of all tests with one SMM ring.

It is helpful to notice that differences in the temperatures between east and west, variations in the time of day when tests were conducted, variations in the measurement of temperature, and the differences in the size and behavior of the firefighters themselves introduce an element of noise into the data. Examining tests which yielded more than a 20% difference in the rate of temperature rise is enlightening because it indicates effects likely to be beyond those of random noise; combining the fall and spring week 2 series yielded 28 tests where the expanding coat had a significantly lower rate of internal temperature rise, in comparison to eight in which the regular did better.

The morning and afternoon tests were also compared. Combining the spring week 2 and fall series reveals that the expanding gear wrought a 33% improvement in the AM tests, but only a 20% average improvement in the afternoon, when the room was generally warmer.

The enhanced gear seemed more effective under, comparatively, milder heat fluxes. The mechanism of activation of the SMM rings requires some time to activate; under higher external heat fluxes, the outer layer will heat more quickly, creating a larger temperature gradient across the coat. The heat flux due to conduction is proportional to the temperature gradient, so the thermal insult to the coat will penetrate more quickly, before the SMM layer has had time to create an insulating air gap.

6. Discussion

6.1 Effectiveness of enhanced gear

The thermally responsive firefighter safety gear was consistently shown to be more effective at insulating its wearers from high heat fluxes associated with fires. By mitigating the heat flux across the gear, it is without question that the gear with shape memory material reduced the temperature rise inside the turnout coat by, on average, 27%, reportedly without increases in bulk or with difficulty handling moisture. It was designed and demonstrated to activate in sufficient time to provide a protective addition of time to the firefighters' maximum comfortable exposures, and the rate at which temperatures increased at the location of the firefighters' cotton shirts decreased remarkably. This effect was most pronounced with the addition of a single layer of expanding ring assembly; a double layer proved to be only marginally more effective than a single at reducing exposure.

The effectiveness of the shape memory material was demonstrated over a wide range of exposure conditions. Applicability to higher and lower heat fluxes suggests that the expanding rings could be effectively implemented in any turnout coat intended to provide thermal insulation against heat, not just the specific design here. This design seemed to be more effective at protecting against lower heat fluxes. In morning tests, before the room heated after several fires, the thermally responsive coat yielded a 33% lower temperature rise than an unaltered coat, in comparison to a 20% in the afternoon tests. The same was true when comparing standing and kneeling tests; the standing tests in the fall showed a 25% difference between regular and expanding coats, in comparison to the kneeling, which yielded a 30% difference. This innovation in thermal protection has wide-ranging ramifications for turnout gear in general, and the potential to save the lives of emergency responders working under extreme conditions.

By maintaining a cooler environment inside the turnout coat, the shape memory rings also created subjectively more comfortable conditions for the firefighters. In so doing, it put them at a reduced risk of hyperthermia and burns, allowing them greater clarity of mind and body inside the burn room. Creating a turnout coat that proves more comfortable will make the firefighters more effective in the performance of fire suppression activities, reducing risk to property and life.

6.2 Future work

Future work on this project should evaluate the effectiveness of the gear for different fits of firefighters, different exposure conditions, and different firefighting activities. More snug fits of gear will tend to restrict the expansion of the shape memory rings; this effect was not characterized in this investigation, but will doubtlessly be important in sizing recommendations for the gear. In addition, the same design fire was used in each run of this experiment. Different exposures could be attempted. The effects of washing the turnout coat must also be investigated.

In future tests, exposure temperature data for the outside of the firefighter coats should be collected to provide more insight into their performance during real exposures. The buttons were utilized in this test to simplify the procedures and to have minimally invasive instrumentation, but different tests in this series could be more effective at collecting data by placing thermocouples on the firefighter turnout coat above where internal temperatures are collected. This could, potentially, be captured by something similar to the buttons used to collect data inside the coat, or by a more complex and portable thermocouple assembly.

Finally, such a gear must be implemented with a caution against use as a license to stay in hot areas longer. Because the gear will be, in general, thicker than gear that does not expand, it will tend to absorb and retain greater amounts of heat, which must be discharged somehow on exit from a fire zone. If a firefighter wears this new gear, he or she must take additional caution to be cognizant of the stored heat inside of the gear; although its effects are remarkable at reducing heat fluxes and at mitigating burn severity, the dangers associated with burns can be even more grave if heat is allowed to build. In implementation of this gear, firefighters could be instructed to consider the relative severity of the heat exposures to which they are subjected, of which the expanding gear may serve as an indicator. This could facilitate their mindfulness of the fire in which they find themselves.

Appendix A: Test Data

Summary test data are presented. The temperature inside the turnout coat was sampled once every two seconds, so the temperature rate of change reported in the table is actually half of the slope of the rate of temperature rise measured from the functions reported subsequently. The exposure temperature was taken as the average of the second highest thermocouple during the exposure.

The graphs showing the button temperature profiles from the spring tests are labeled with the names of each of the tests to which they correspond.

date	am/pm	dT/dt				East exposure (C)	West exposure (C)
		A	B	C	D		
28-Nov	am	0.14	0.165	0.125	0.165	320	270
	am	0.125	0.12	0.215	0.225	370	260
	pm	0.2	0.275	0.28	0.29	450	450
	pm	0.27	0.25	0.14	0.255	440	390
29-Nov	am	0.13	0.1	0.11	0.085	360	380
	am	0.115	0.095	0.19	0.175	370	450
	pm	0.07	0.095	0.08	0.1	510	400
	pm	0.05	0.07	0.095	0.075	320	290
30-Nov	am	0.27	0.31	0.22	0.14	450	360
	am	0.26	0.19	0.27	0.19	460	340
	pm	0.25	0.22	0.23	0.15	510	420
	pm	0.34	0.28	0.19	0.22	510	390
1-Dec	am	0.14	0.17	0.11	0.13	380	190
	am	0.14	0.12	0.06	0.09	340	270

	am	0.12	0.12	0.18	0.15	290	260
	am	0.12	0.08	0.1	0.14	500	375
	pm	0.18	0.21	0.26	0.22	545	440
	pm	0.21	0.25	0.16	0.31	580	450
2-Dec	**am**	0.26	0.24	0.105	0.15	480	340
	am	0.175	0.14	0.165	0.11	430	350
	pm	0.125	0.12	0.225	0.27	470	390
	pm	0.125	0.13	0.115	0.2	540	540
5-Dec	**am**	0.245	0.14	0.08	0.12	420	360
	am	0.12	0.09	0.11	0.13	380	340
	pm	0.13	0.11	0.115	0.125	540	460
	pm	0.1	0.12	0.08	0.12	520	470
6-Dec	**am**	0.235	0.225	0.15	0.12	490	380
	am	0.24	0.15	0.24	0.115	xx	xx
	pm	0.17	0.135	0.27	0.11	430	420
	pm	0.195	0.18	0.155	0.075	530	480
7-Dec	**am**	0.085	0.08	0.07	0.07	490	390
	am	0.08	0.105	0.1	0.075	380	290
8-Dec	**am**	0.175	0.25	0.21	0.25	450	370
	am	0.13	0.245	0.385	0.225	470	400
	pm	0.215	0.225	0.315	0.365	430	430
	pm	0.355	0.2	0.305	0.325	560	520
9-Dec	**am**	0.115	0.095	0.09	0.09	470	370
	am	0.195	0.14	0.19	0.25	440	360
	pm	0.21	0.13	0.17	0.235	580	470

	pm	0.255	0.18	0.115	0.17	520	440
26-Mar	**am**	0.17	0.11	0.2	0.21		
26-Mar	**am**	0.07	0.06	0.07	0.12		
26-Mar	**pm**	0.125	0.093	0.08	0.14		
26-Mar	**pm**	0.093	0.12	0.06	0.14		
27-Mar	**am**	0.12	0.11	0.1	0.09		
27-Mar	**am**	0.11	0.1	0.13	0.14		
27-Mar	**pm**	0.11	0.08	0.1	0.12		
27-Mar	**pm**	0.1	0.09	0.11	0.12		
28-Mar	**am**	0.19	0.12	0.07	0.07		
28-Mar	**am**	0.23	0.11	0.08	0.11		
28-Mar	**pm**	0.22	0.26	0.1	0.15		
28-Mar	**pm**	0.15	0.1	0.12	0.08		
29-Mar	**am**	0.09	0.14	0.08	0.09		
29-Mar	**am**	0.11	0.11	0.06	0.07		
29-Mar	**pm**	0.12	0.14	0.08	0.1		
29-Mar	**pm**	0.15	0.17	0.08	0.1		
30-Mar	**am**	0.17	0.21	0.18	0.19		
30-Mar	**am**	0.14	0.1	0.11	0.14		
30-Mar	**pm**	0.13	0.13	0.13	0.21		
30-Mar	**pm**	0.13	0.14	0.1	0.1		
2-Apr	**am**	0.06	0.05	0.1	0.08	410	320
2-Apr	**am**	0.08	0.05	0.12	0.1	560	380
2-Apr	**pm**	0.14	0.07	0.18	0.16	500	420

2-Apr	**pm**	0.1	0.06	0.13	0.06	370	310
3-Apr	**am**	0.13	0.31	0.2	0.25	550	490
3-Apr	**am**	0.21	0.21	0.17	0.1	720	580
3-Apr	**pm**	0.41	0.2	0.26	0.23	570	460
3-Apr	**pm**	0.37	0.22	0.24	0.1	450	350
4-Apr	**am**	0.21	0.29	0.08	0.12	470	380
4-Apr	**am**	0.17	0.09	0.09	0.12	410	370
4-Apr	**pm**	0.13	0.2	0.13	0.1	410	330
4-Apr	**pm**	0.06	0.08	0.07	0.09	340	310
5-Apr	**am**	0.27	0.22	0.2	0.32	320	280
5-Apr	**am**	0.1	0.12	0.15	0.23	370	320
5-Apr	**pm**	0.25	0.26	0.24	0.42	430	380
5-Apr	**pm**	0.24	0.18	0.09	0.26	400	310
6-Apr	**am**	0.18	0.12	0.25	0.22	540	590
6-Apr	**am**	0.1	0.18	0.26	0.33	190	260
6-Apr	**pm**	0.1	0.06	0.18	0.18	290	150
6-Apr	**pm**	0.16	0.11	0.25	0.26	390	240

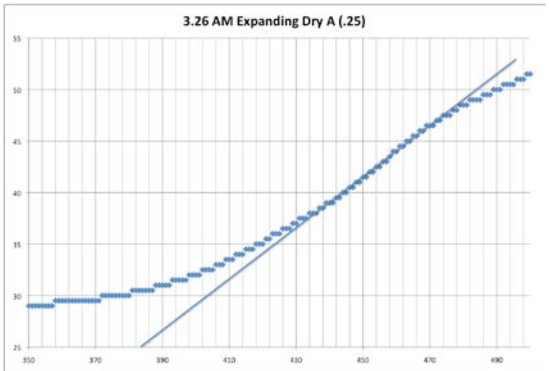
3.26 AM Expanding Dry A (.25)

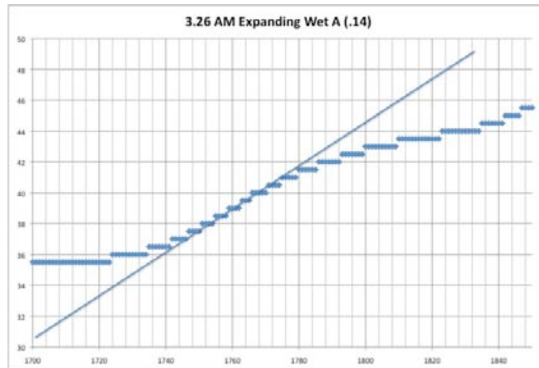
3.26 AM Expanding Wet A (.14)

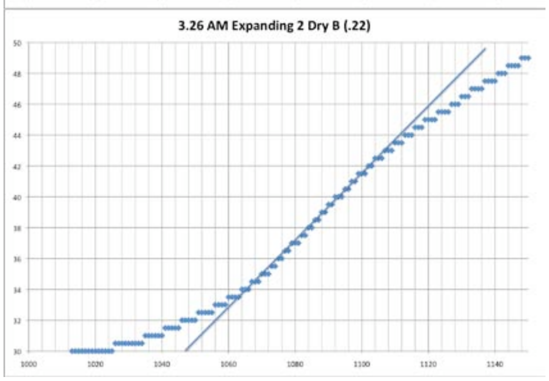
3.26 AM Expanding 2 Dry B (.22)

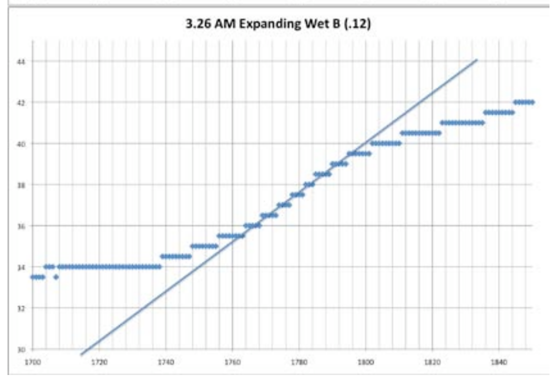
3.26 AM Expanding Wet B (.12)

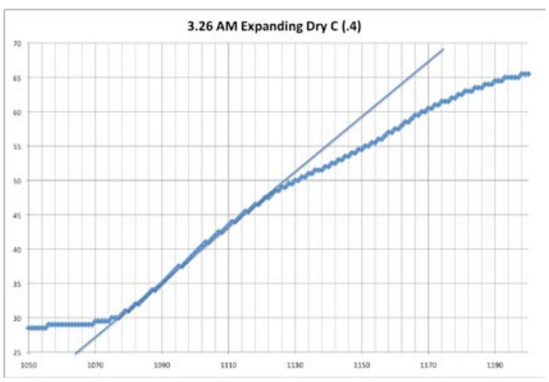
3.26 AM Expanding Dry C (.4)

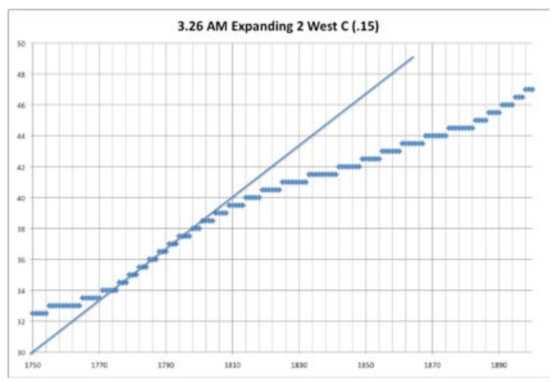
3.26 AM Expanding 2 West C (.15)

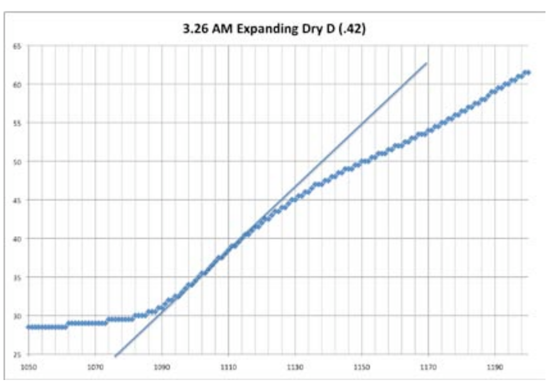
3.26 AM Expanding Dry D (.42)

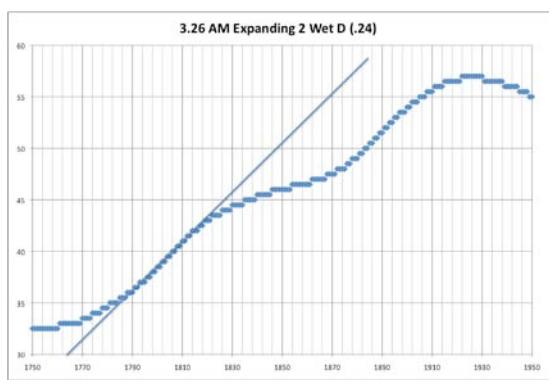
3.26 AM Expanding 2 Wet D (.24)

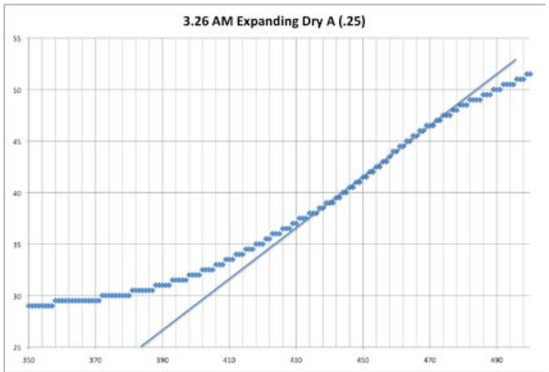
3.26 AM Expanding Dry A (.25)

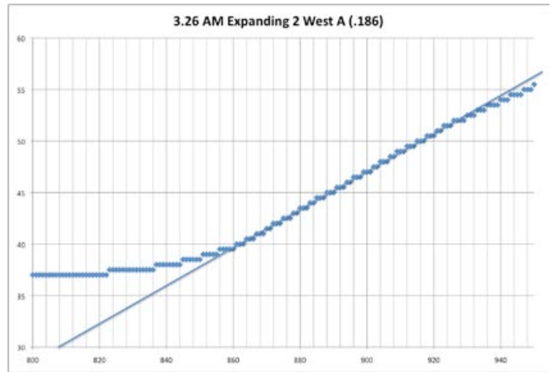
3.26 AM Expanding 2 West A (.186)

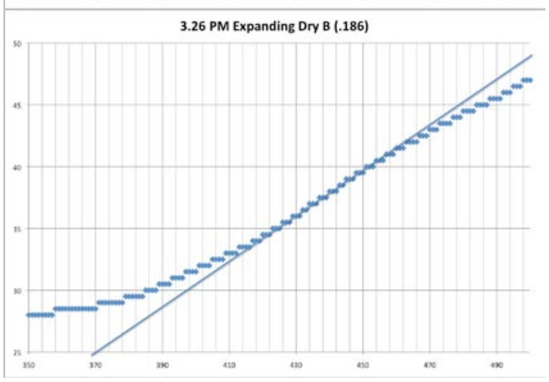
3.26 PM Expanding Dry B (.186)

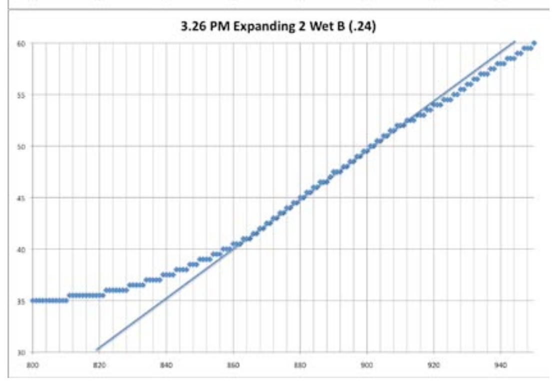
3.26 PM Expanding 2 Wet B (.24)

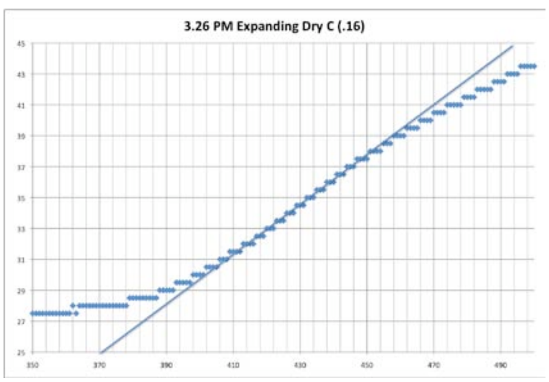
3.26 PM Expanding Dry C (.16)

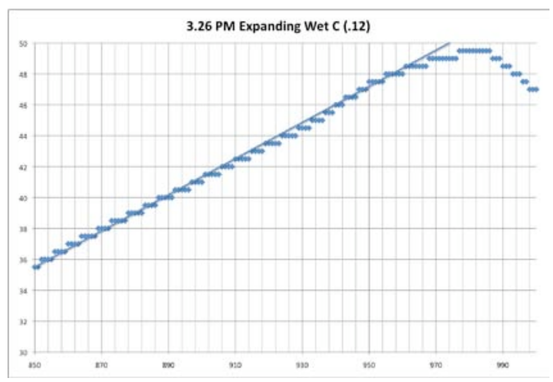
3.26 PM Expanding Wet C (.12)

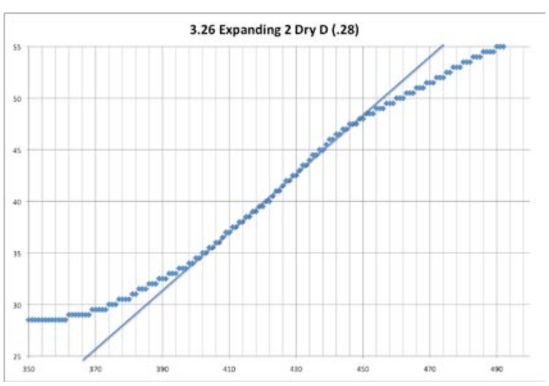
3.26 Expanding 2 Dry D (.28)

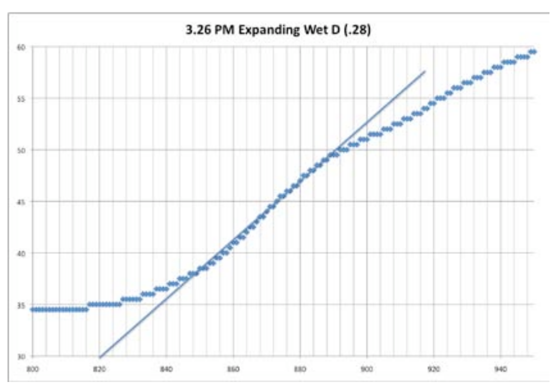
3.26 PM Expanding Wet D (.28)

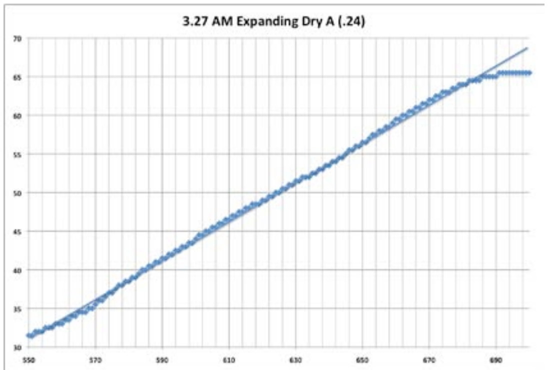
3.27 AM Expanding Dry A (.24)

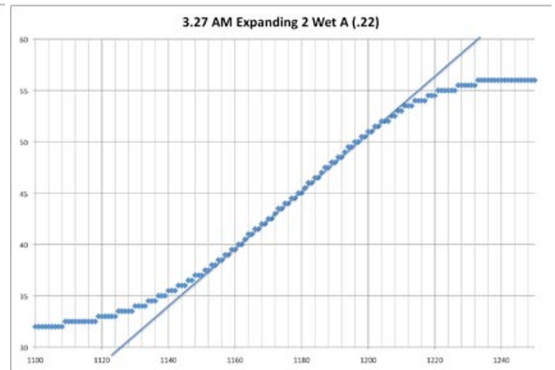
3.27 AM Expanding 2 Wet A (.22)

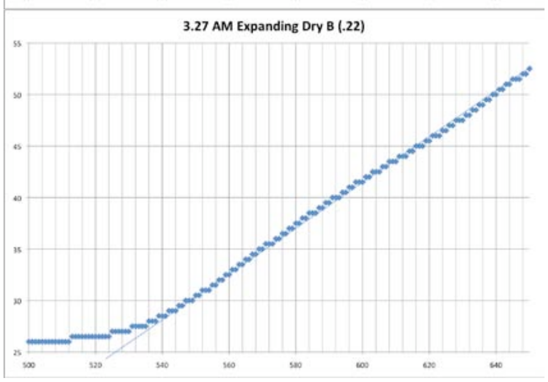
3.27 AM Expanding Dry B (.22)

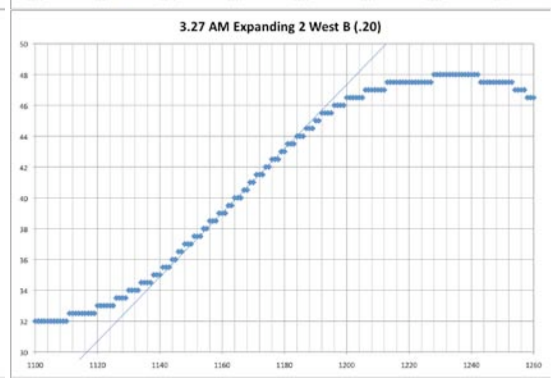
3.27 AM Expanding 2 West B (.20)

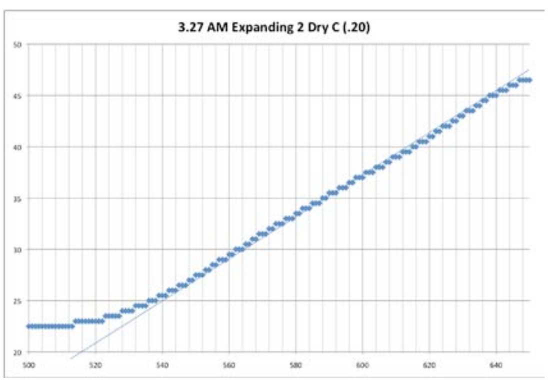
3.27 AM Expanding 2 Dry C (.20)

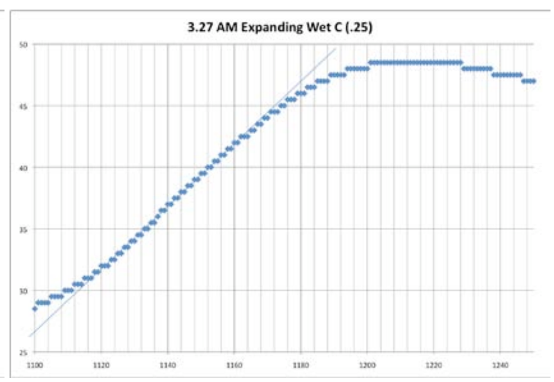
3.27 AM Expanding Wet C (.25)

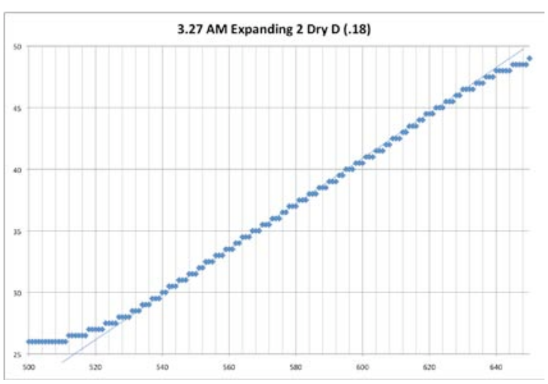
3.27 AM Expanding 2 Dry D (.18)

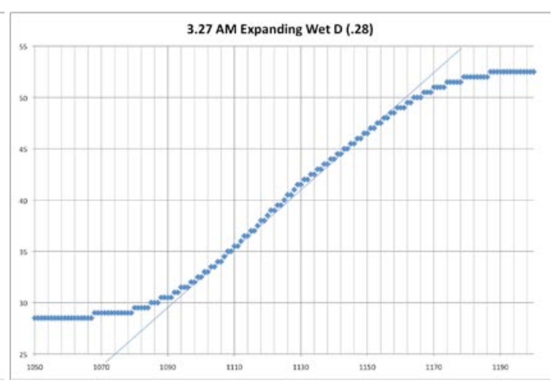
3.27 AM Expanding Wet D (.28)

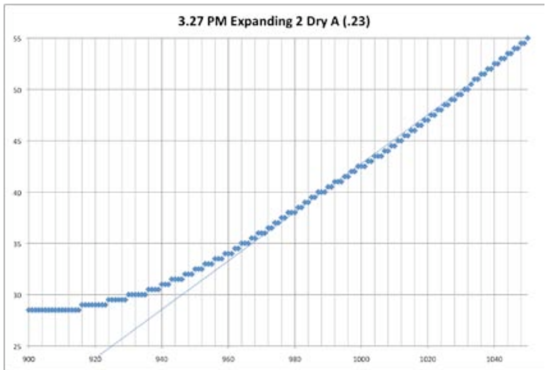
3.27 PM Expanding 2 Dry A (.23)

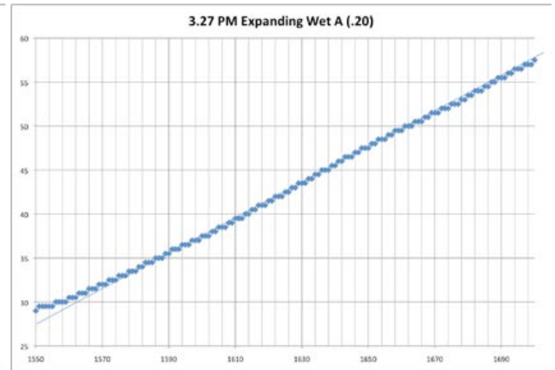
3.27 PM Expanding Wet A (.20)

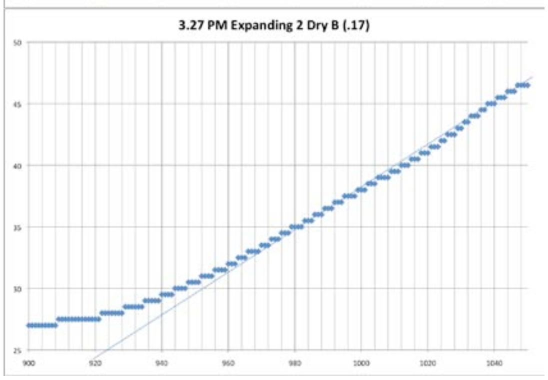
3.27 PM Expanding 2 Dry B (.17)

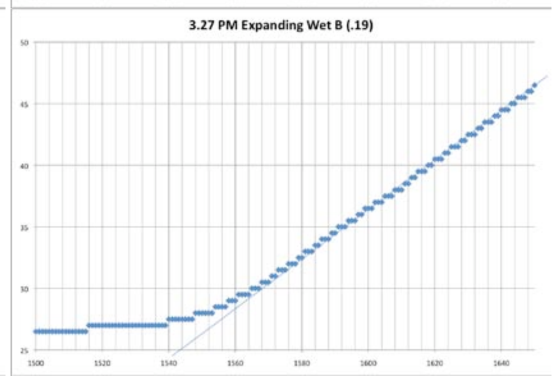
3.27 PM Expanding Wet B (.19)

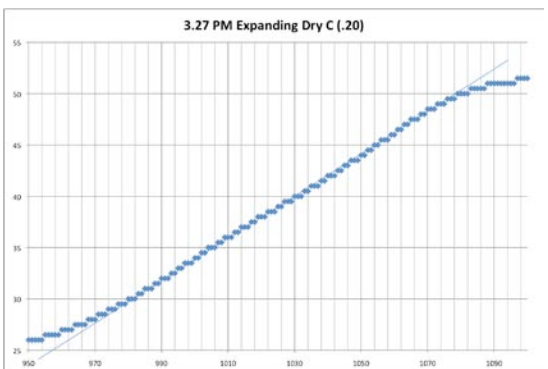
3.27 PM Expanding Dry C (.20)

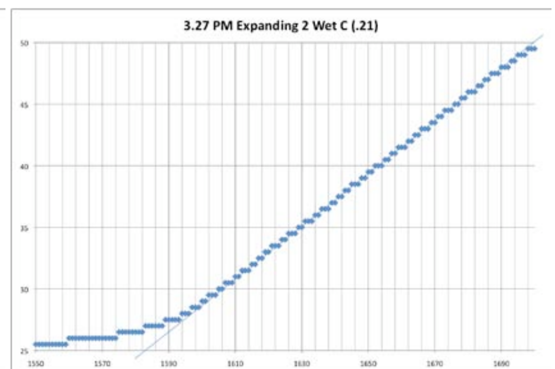
3.27 PM Expanding 2 Wet C (.21)

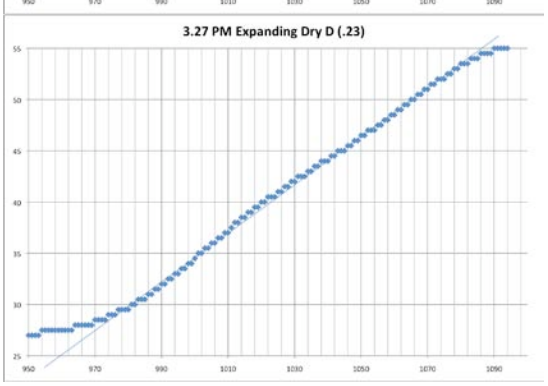
3.27 PM Expanding Dry D (.23)

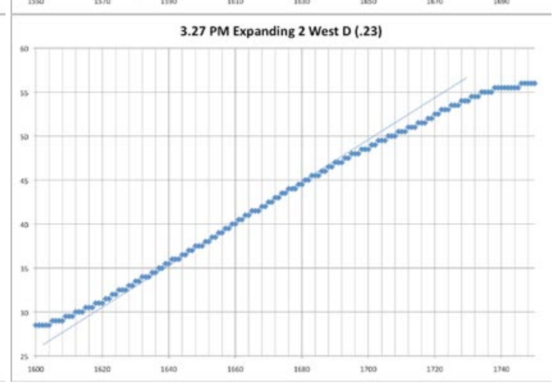
3.27 PM Expanding 2 West D (.23)

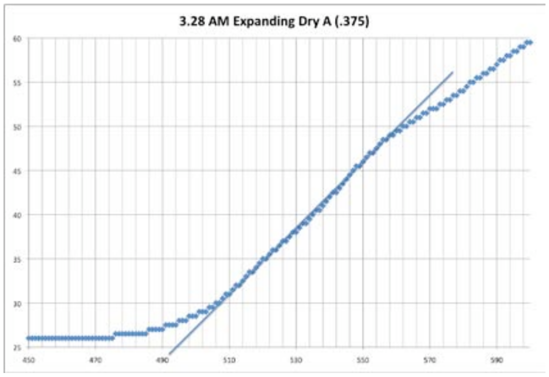
3.28 AM Expanding Dry A (.375)
60
55
50
45
40
35
30
25
450
470
490
510
530
550
570
590

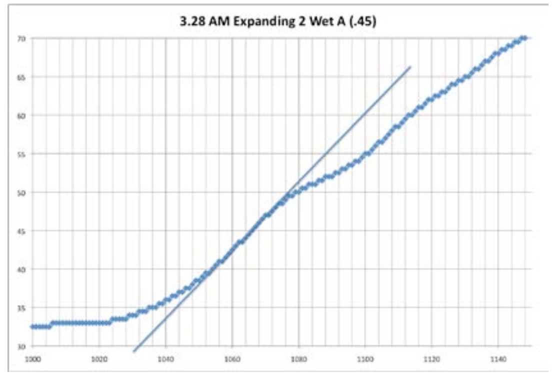
3.28 AM Expanding 2 Wet A (.45)
70
65
60
55
50
45
40
35
30
1000
1020
1040
1060
1080
1100
1120
1140

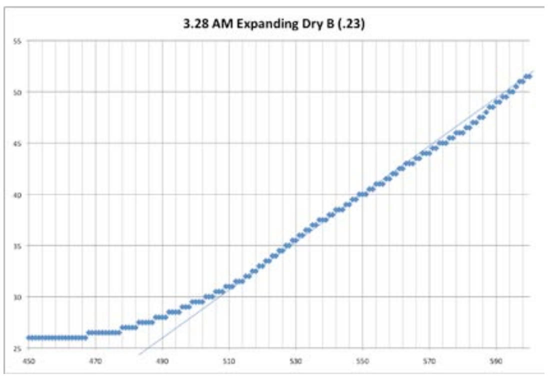
3.28 AM Expanding Dry B (.23)
55
50
45
40
35
30
25
450
470
490
510
530
550
570
590

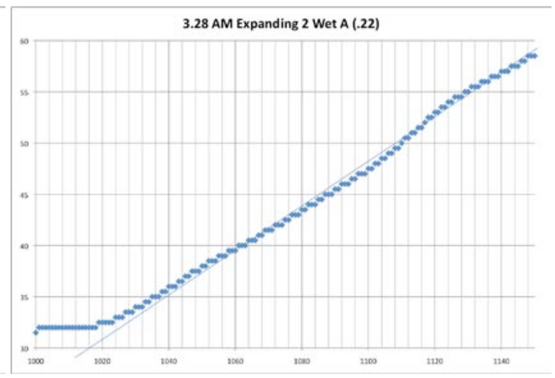
3.28 AM Expanding 2 Wet A (.22)
60
55
50
45
40
35
30
1000
1020
1040
1060
1080
1100
1120
1140

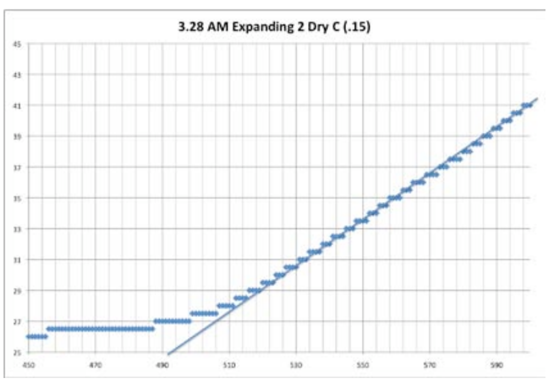
3.28 AM Expanding 2 Dry C (.15)
45
43
41
39
37
35
33
31
29
27
25
450
470
490
510
530
550
570
590

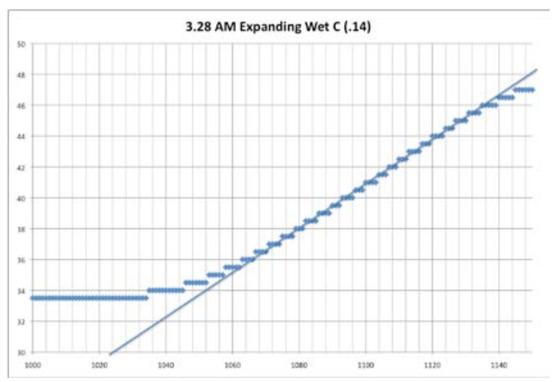
3.28 AM Expanding Wet C (.14)
50
48
46
44
42
40
38
36
34
32
30
1000
1020
1040
1060
1080
1100
1120
1140

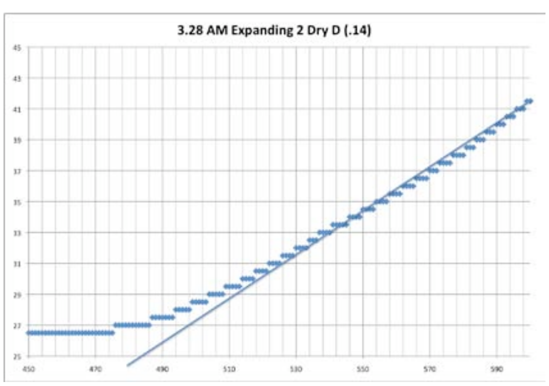
3.28 AM Expanding 2 Dry D (.14)
45
43
41
39
37
35
33
31
29
27
25
450
470
490
510
530
550
570
590

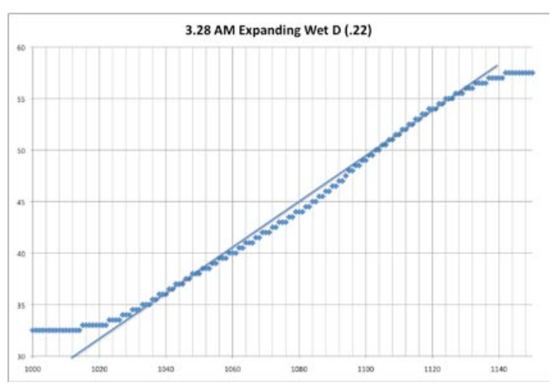
3.28 AM Expanding Wet D (.22)
60
55
50
45
40
35
30
1000
1020
1040
1060
1080
1100
1120
1140

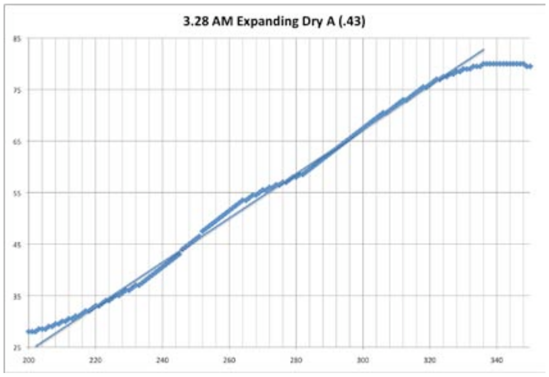
3.28 AM Expanding Dry A (.43)
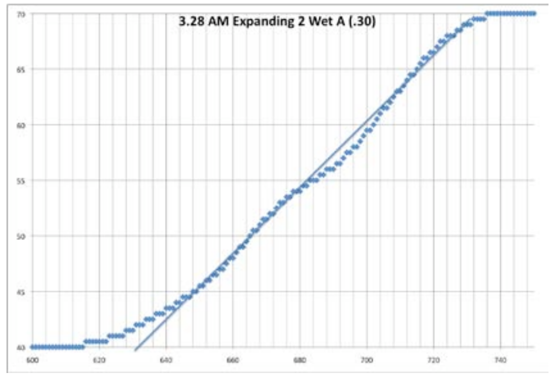
3.28 AM Expanding 2 Wet A (.30)
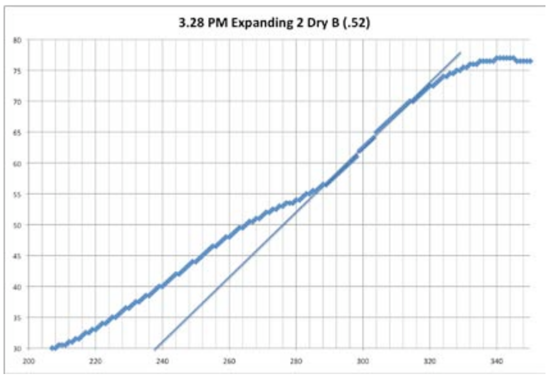
3.28 PM Expanding 2 Dry B (.52)
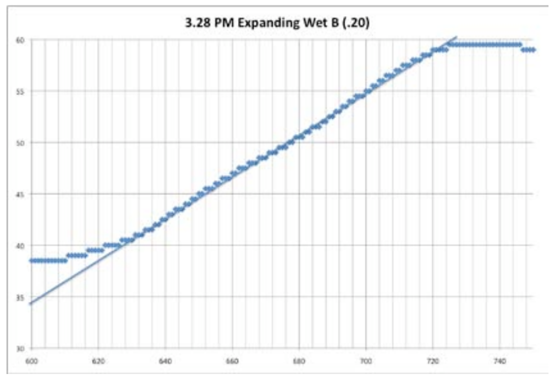
3.28 PM Expanding Wet B (.20)
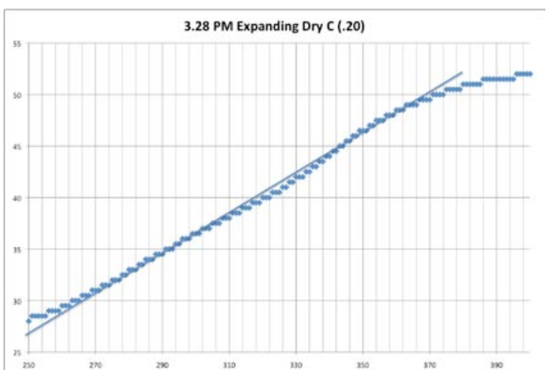
3.28 PM Expanding Dry C (.20)
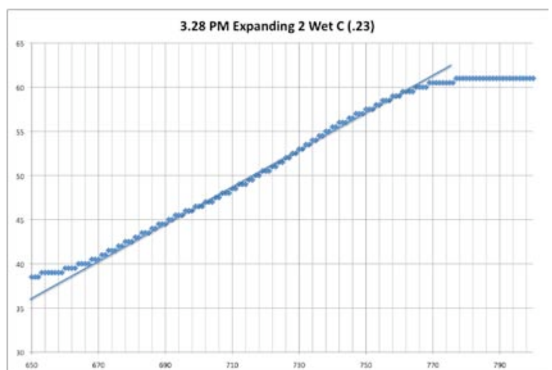
3.28 PM Expanding 2 Wet C (.23)
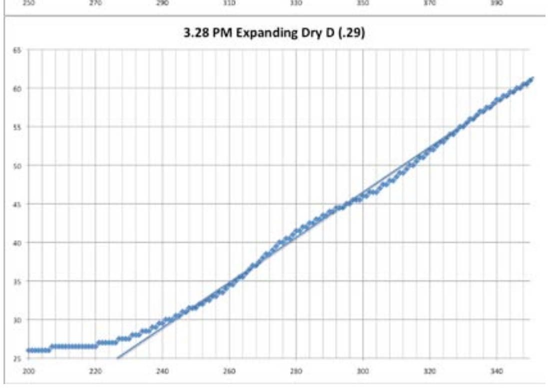
3.28 PM Expanding Dry D (.29)
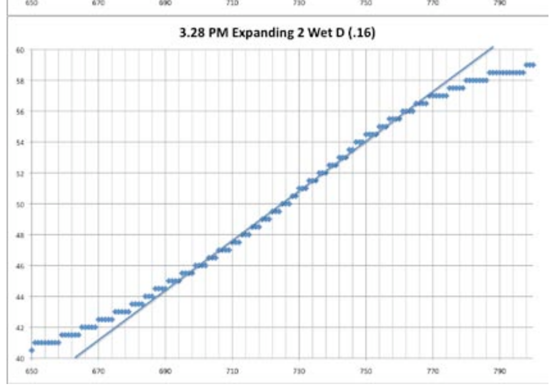
3.28 PM Expanding 2 Wet D (.16)

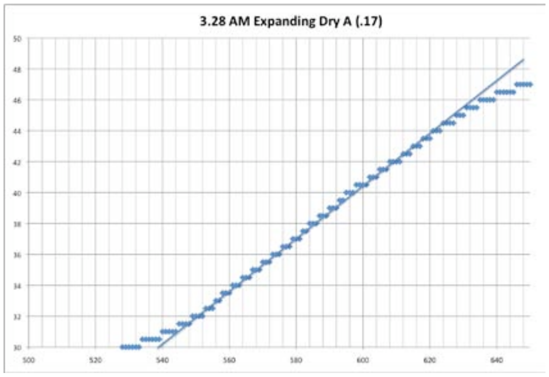
3.28 AM Expanding Dry A (.17)

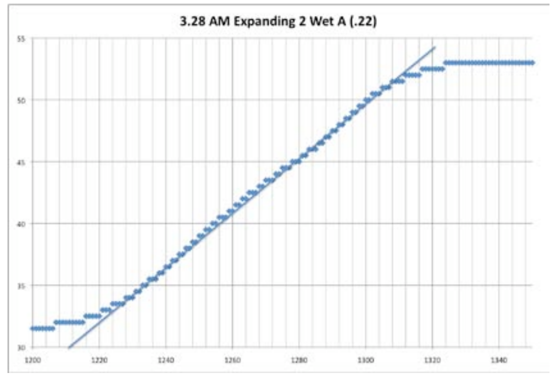
3.28 AM Expanding 2 Wet A (.22)

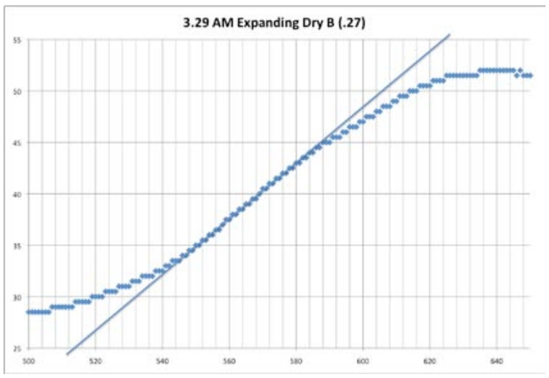
3.29 AM Expanding Dry B (.27)

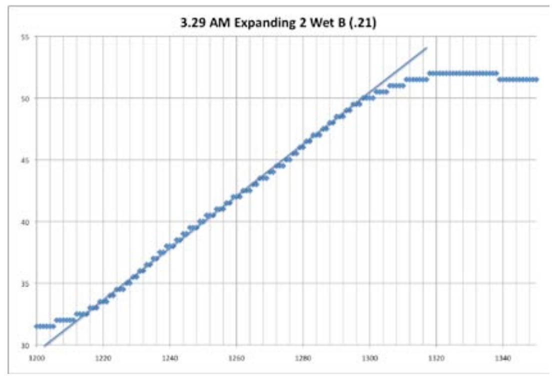
3.29 AM Expanding 2 Wet B (.21)

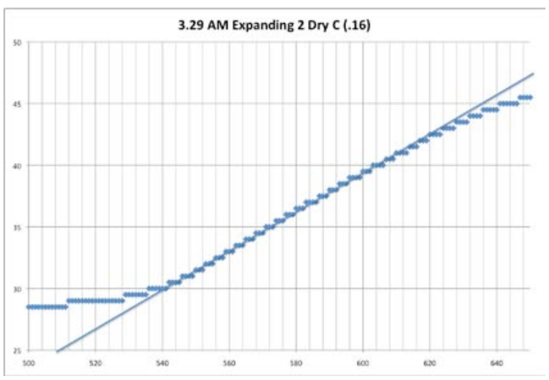
3.29 AM Expanding 2 Dry C (.16)

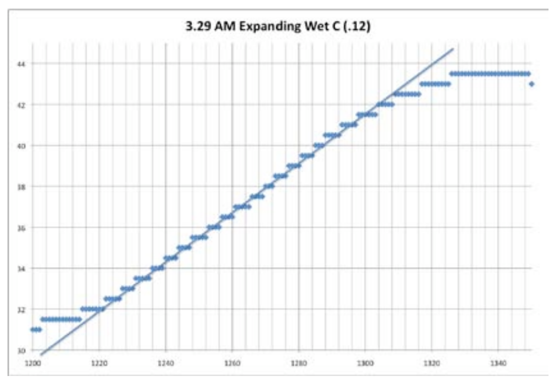
3.29 AM Expanding Wet C (.12)

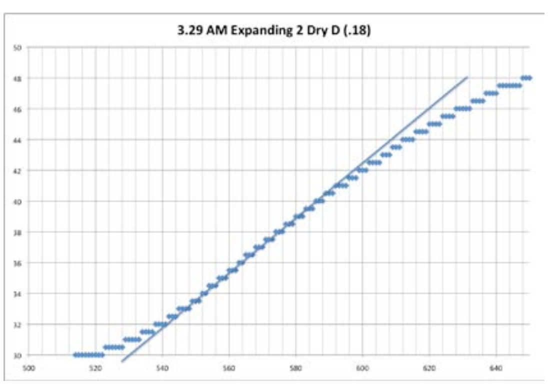
3.29 AM Expanding 2 Dry D (.18)

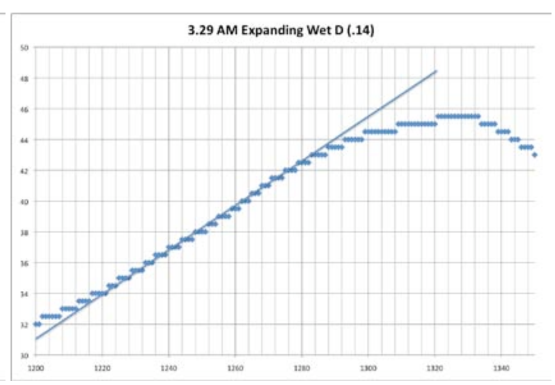
3.29 AM Expanding Wet D (.14)

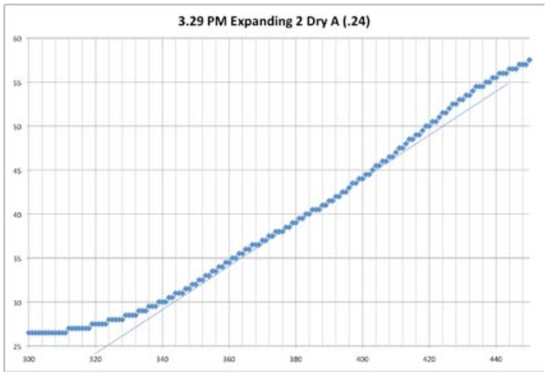
3.29 PM Expanding 2 Dry A (.24)

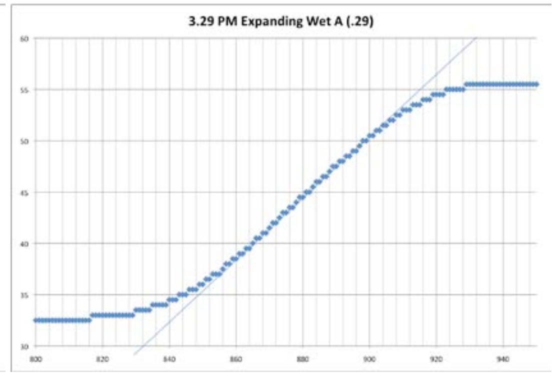
3.29 PM Expanding Wet A (.29)

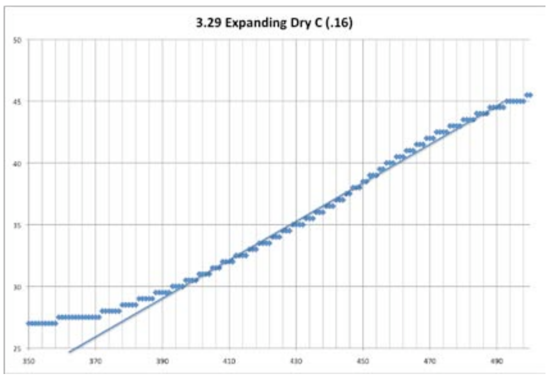
3.29 Expanding Dry C (.16)

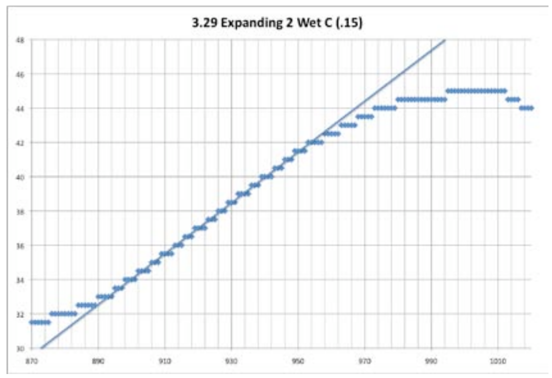
3.29 Expanding 2 Wet C (.15)

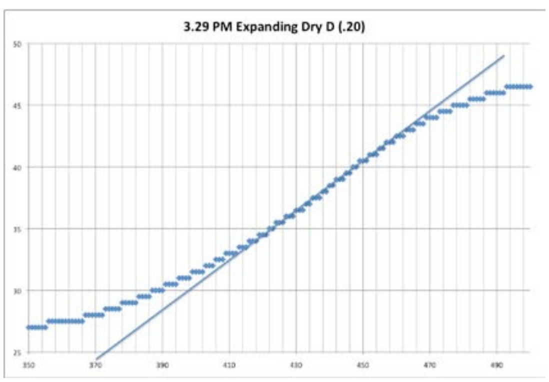
3.29 PM Expanding Dry D (.20)

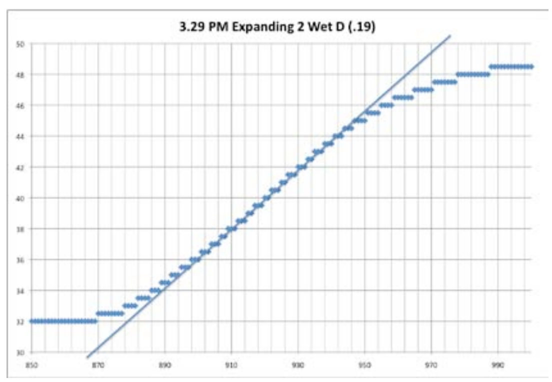
3.29 PM Expanding 2 Wet D (.19)

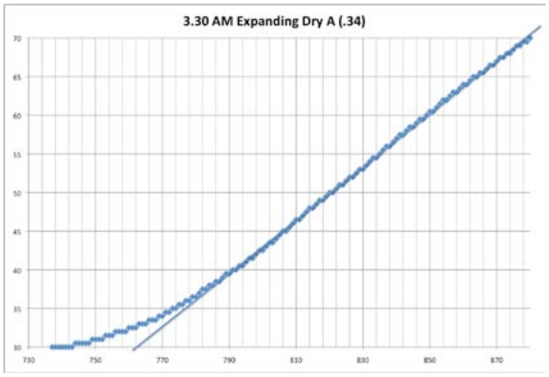
3.30 AM Expanding Dry A (.34)
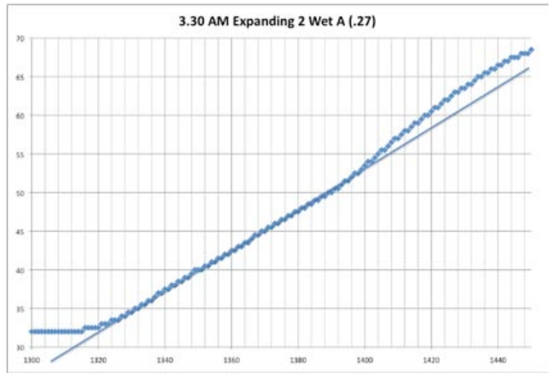
3.30 AM Expanding 2 Wet A (.27)
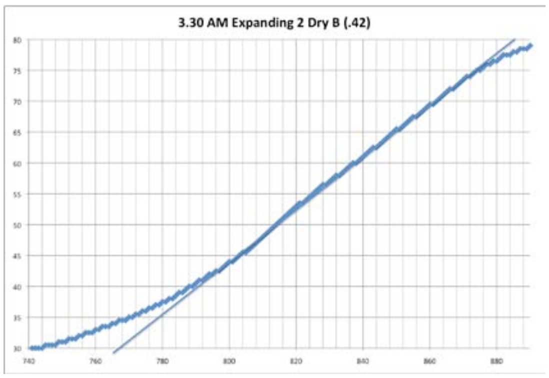
3.30 AM Expanding 2 Dry B (.42)
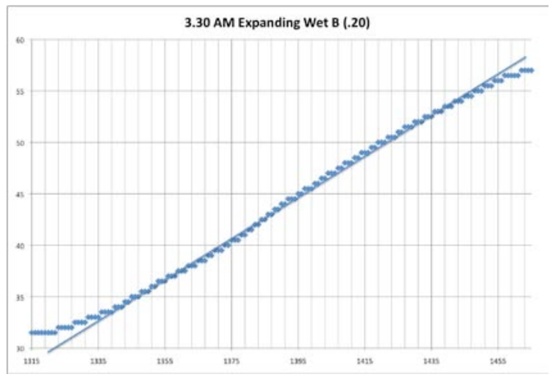
3.30 AM Expanding Wet B (.20)
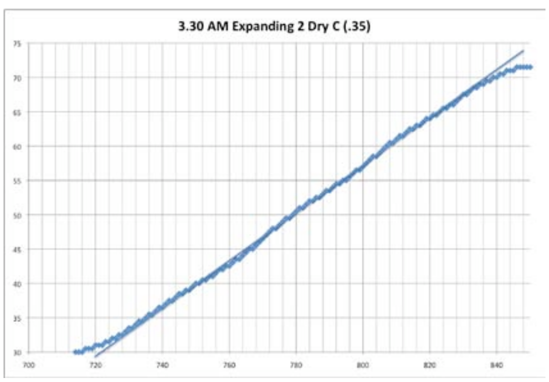
3.30 AM Expanding 2 Dry C (.35)
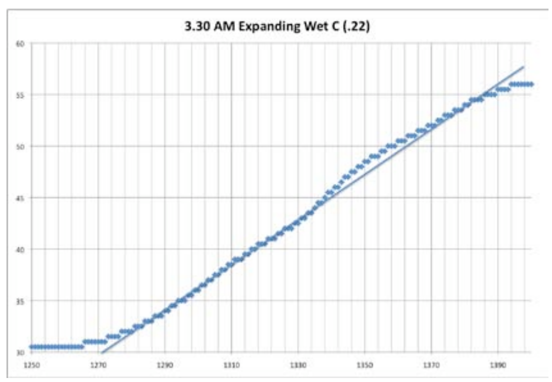
3.30 AM Expanding Wet C (.22)
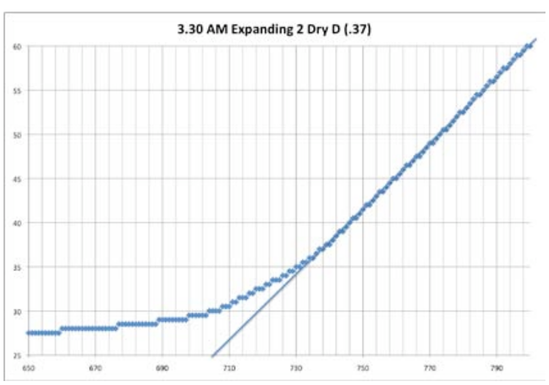
3.30 AM Expanding 2 Dry D (.37)
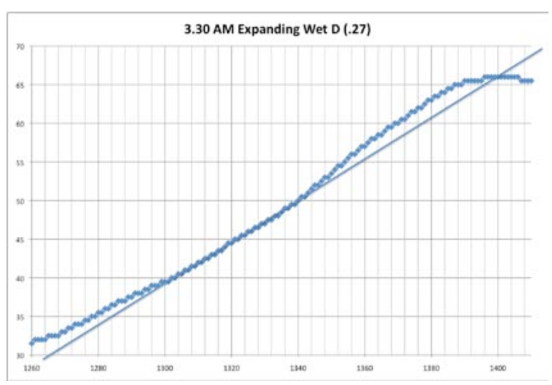
3.30 AM Expanding Wet D (.27)

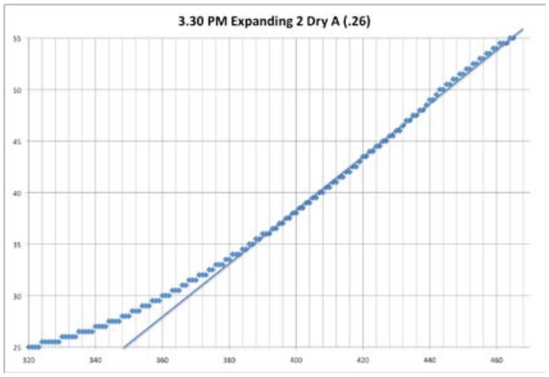
3.30 PM Expanding 2 Dry A (.26)

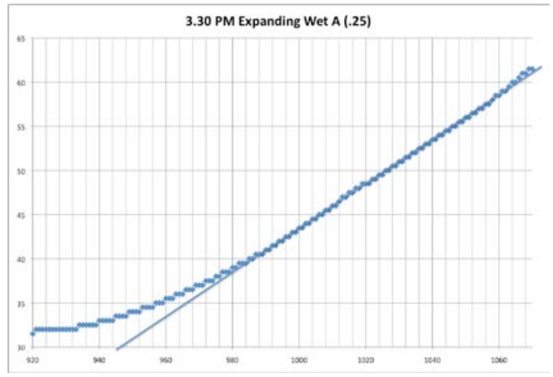
3.30 PM Expanding Wet A (.25)

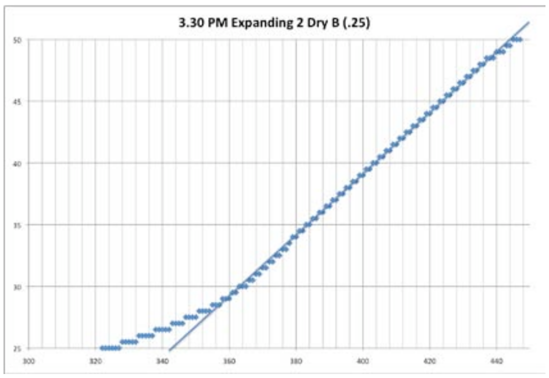
3.30 PM Expanding 2 Dry B (.25)

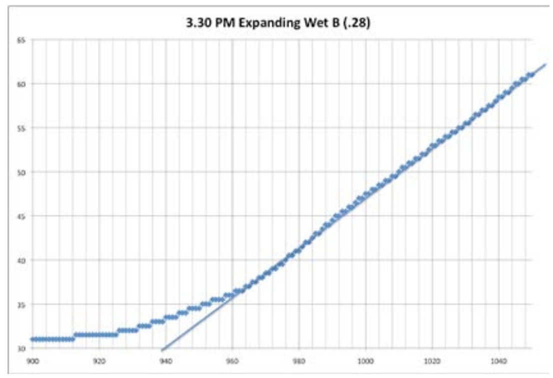
3.30 PM Expanding Wet B (.28)

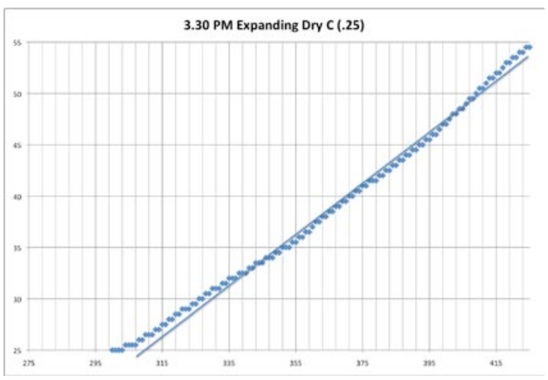
3.30 PM Expanding Dry C (.25)

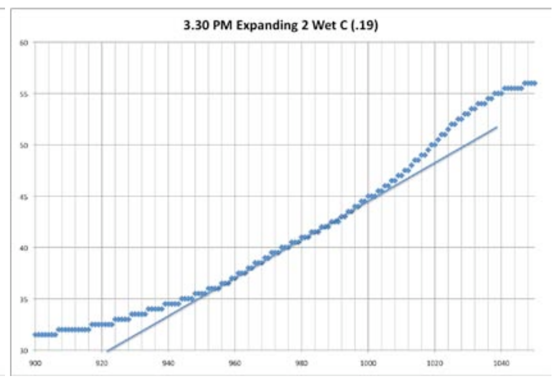
3.30 PM Expanding 2 Wet C (.19)

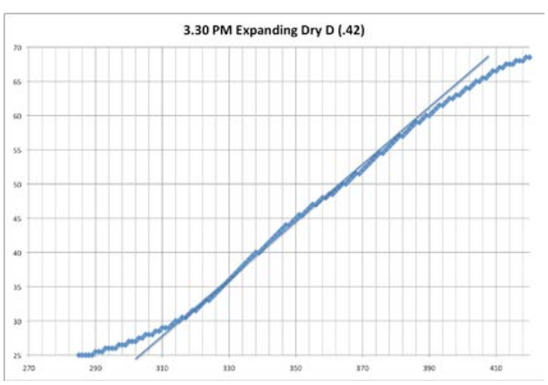
3.30 PM Expanding Dry D (.42)

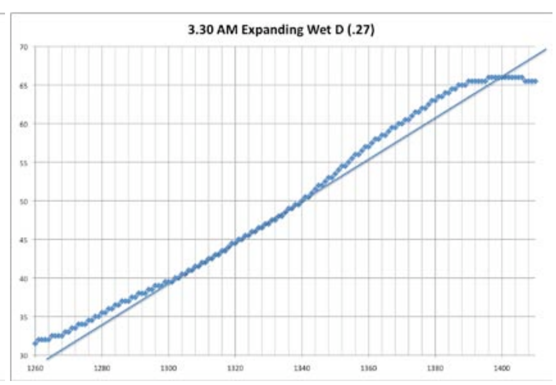
3.30 AM Expanding Wet D (.27)

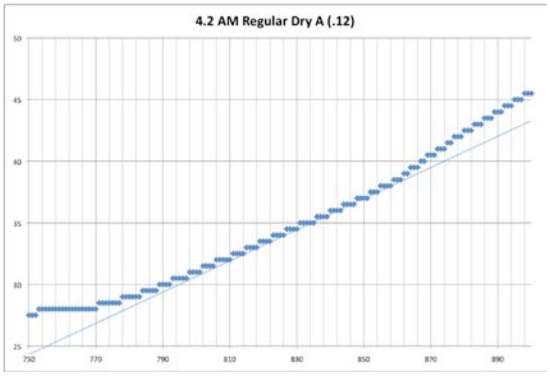
4.2 AM Regular Dry A (.12)

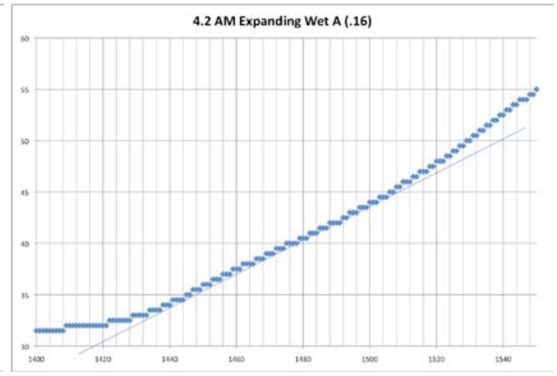
4.2 AM Expanding Wet A (.16)

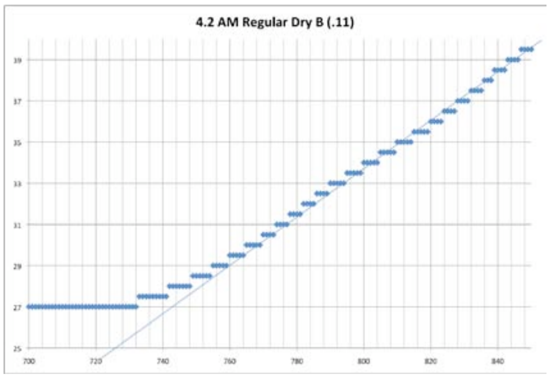
4.2 AM Regular Dry B (.11)

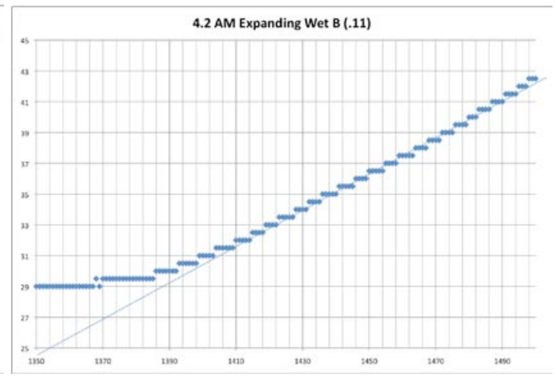
4.2 AM Expanding Wet B (.11)

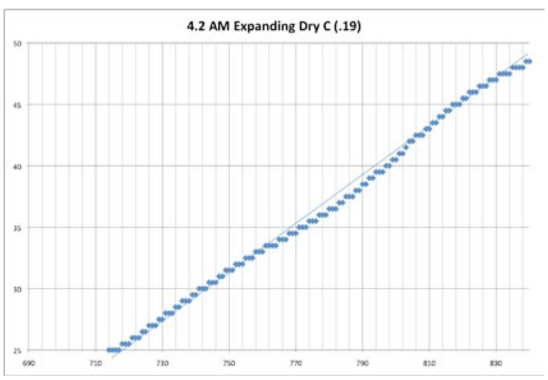
4.2 AM Expanding Dry C (.19)

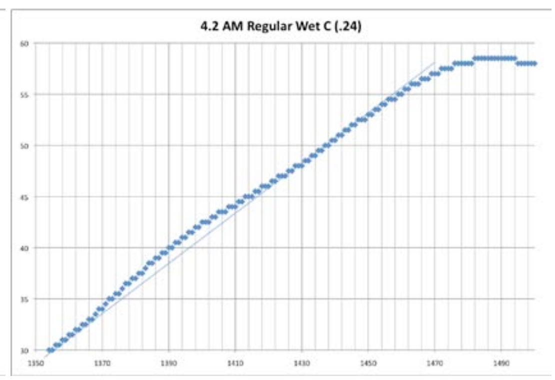
4.2 AM Regular Wet C (.24)

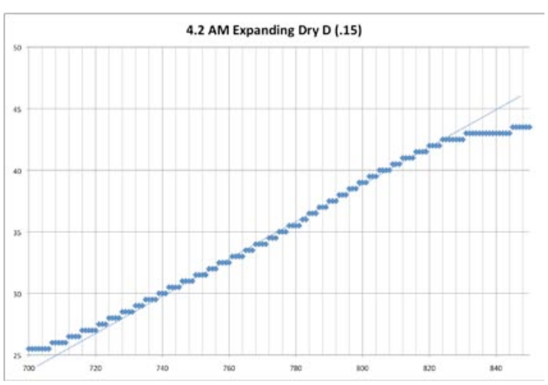
4.2 AM Expanding Dry D (.15)

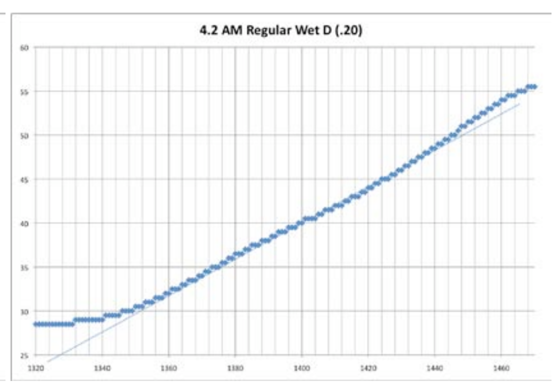
4.2 AM Regular Wet D (.20)

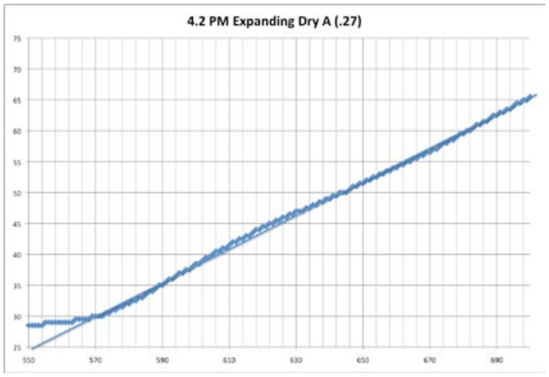
4.2 PM Expanding Dry A (.27)

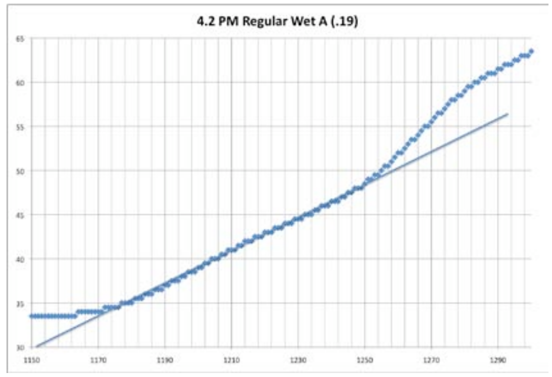
4.2 PM Regular Wet A (.19)

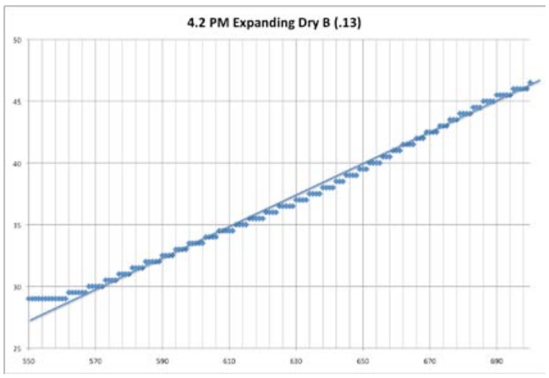
4.2 PM Expanding Dry B (.13)

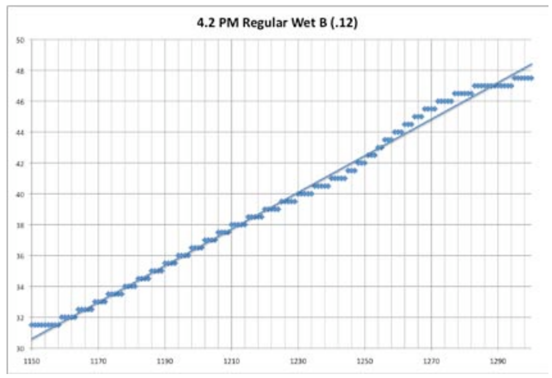
4.2 PM Regular Wet B (.12)

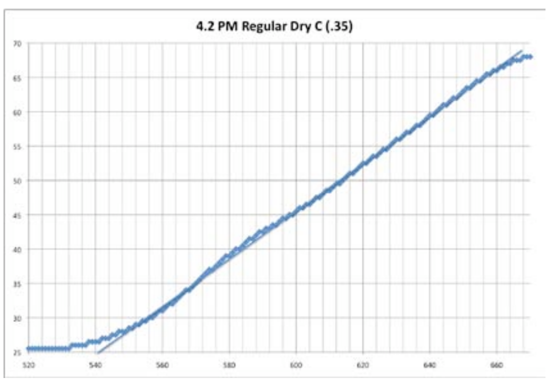
4.2 PM Regular Dry C (.35)

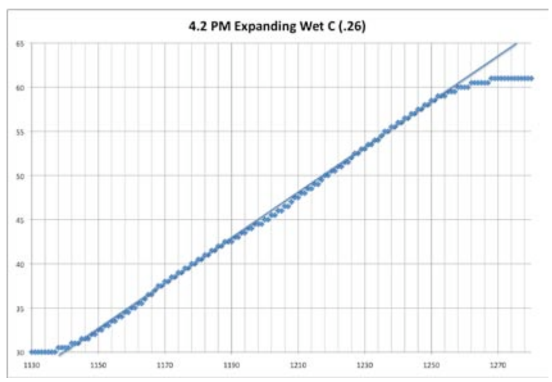
4.2 PM Expanding Wet C (.26)

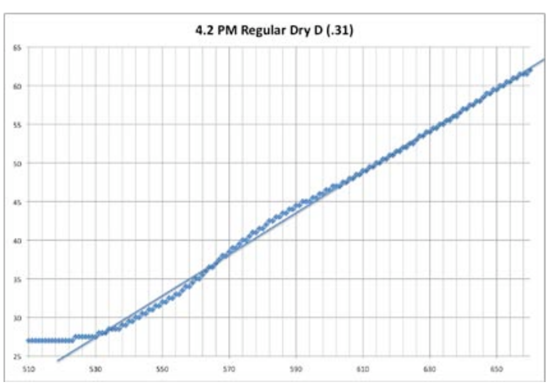
4.2 PM Regular Dry D (.31)

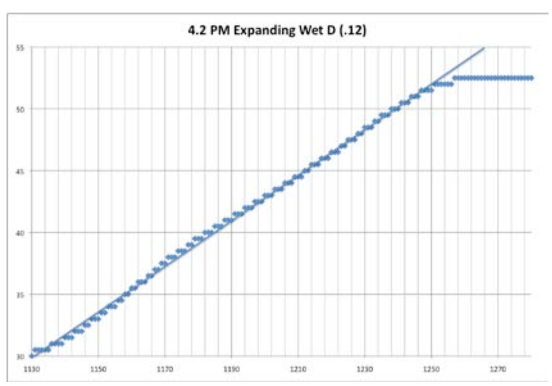
4.2 PM Expanding Wet D (.12)

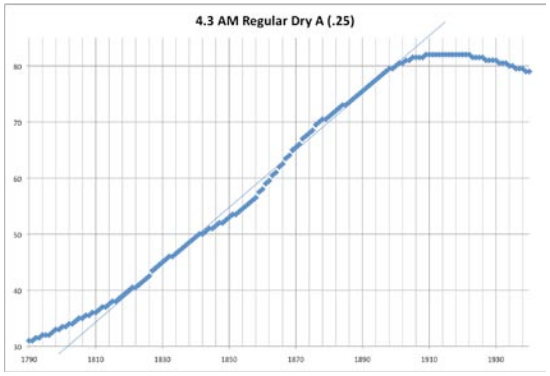
4.3 AM Regular Dry A (.25)

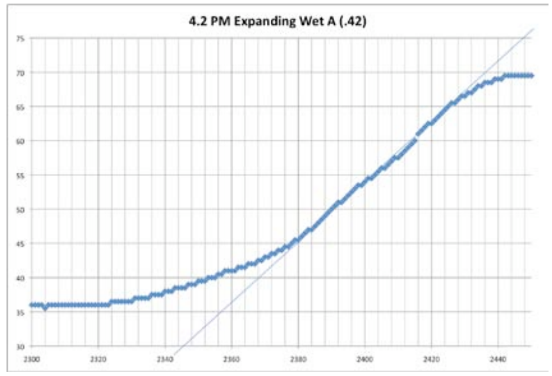
4.2 PM Expanding Wet A (.42)

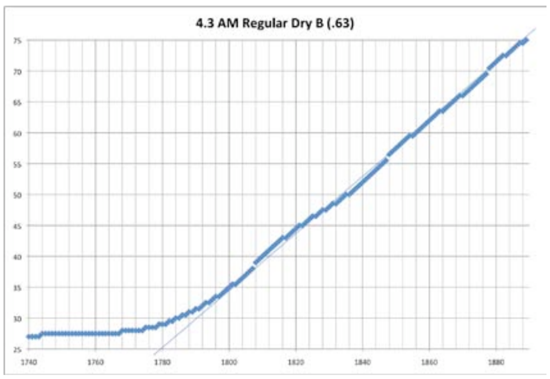
4.3 AM Regular Dry B (.63)

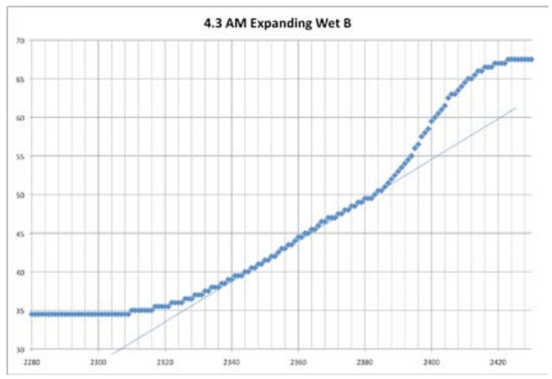
4.3 AM Expanding Wet B

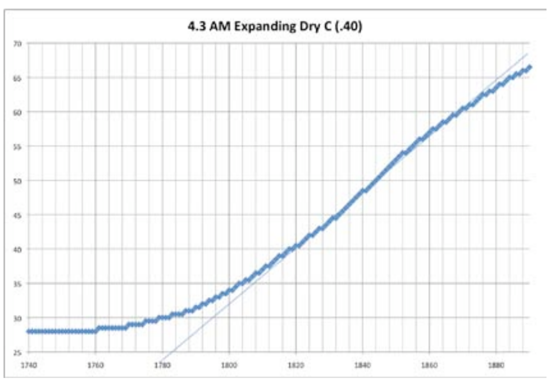
4.3 AM Expanding Dry C (.40)

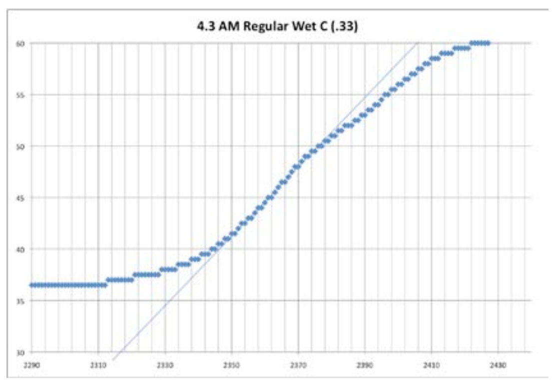
4.3 AM Regular Wet C (.33)

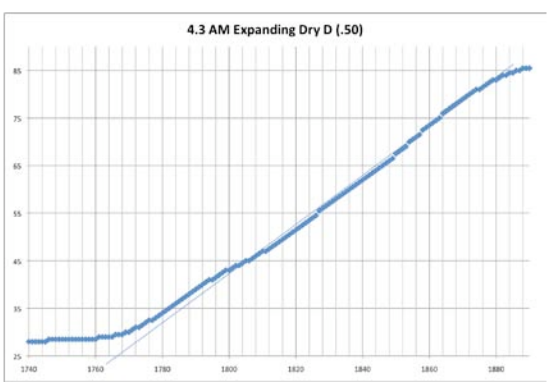
4.3 AM Expanding Dry D (.50)

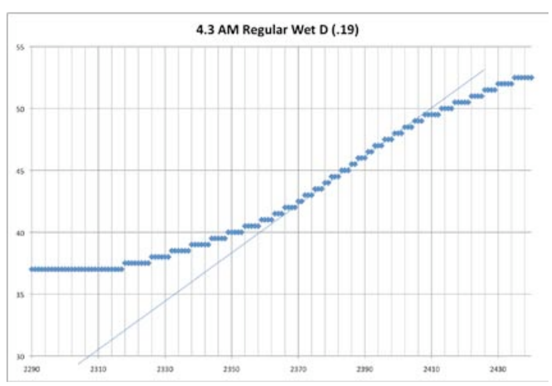
4.3 AM Regular Wet D (.19)

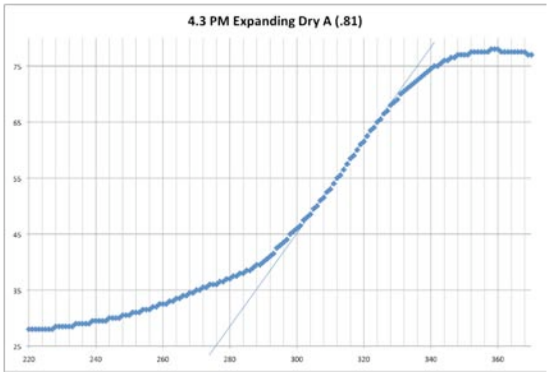
4.3 PM Expanding Dry A (.81)

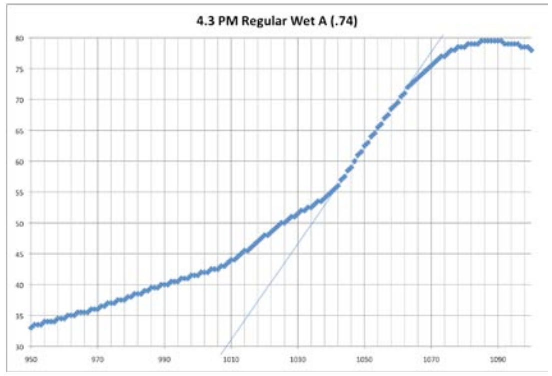
4.3 PM Regular Wet A (.74)

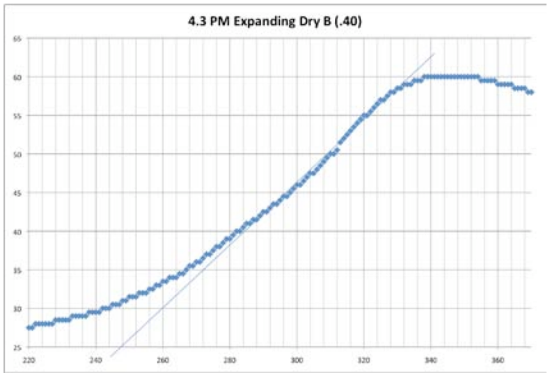
4.3 PM Expanding Dry B (.40)

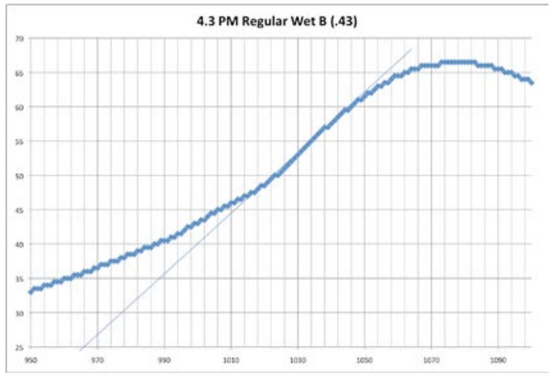
4.3 PM Regular Wet B (.43)

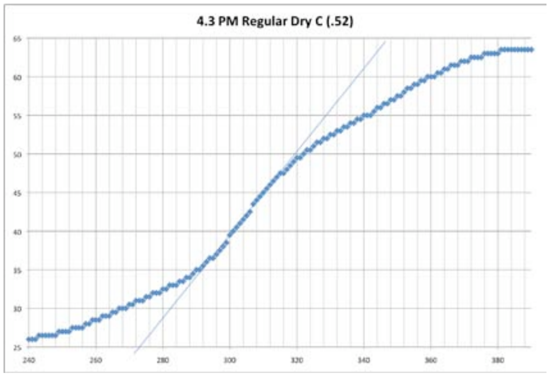
4.3 PM Regular Dry C (.52)

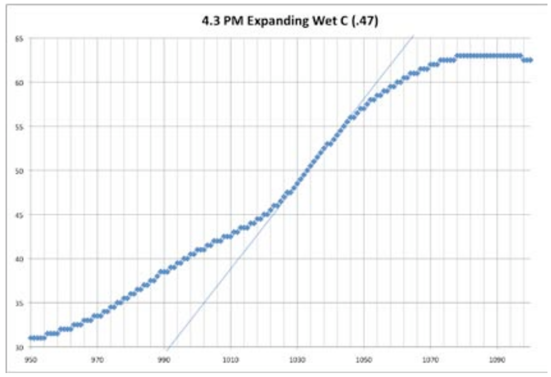
4.3 PM Expanding Wet C (.47)

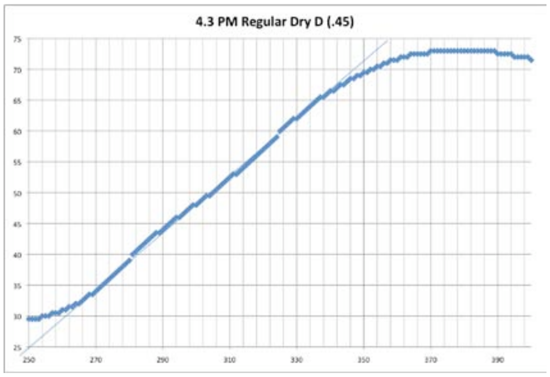
4.3 PM Regular Dry D (.45)

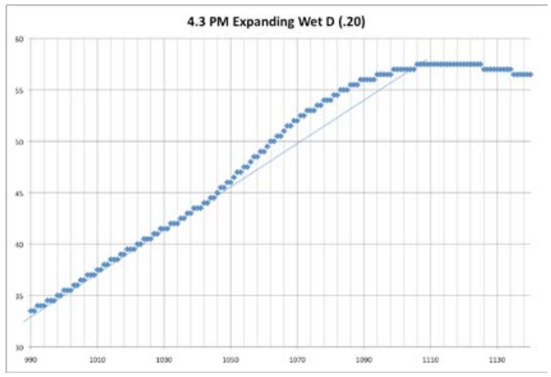
4.3 PM Expanding Wet D (.20)

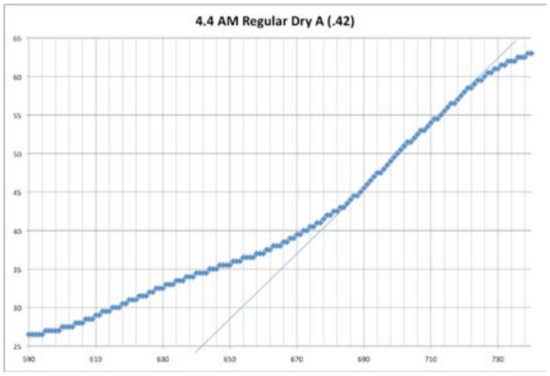
4.4 AM Regular Dry A (.42)

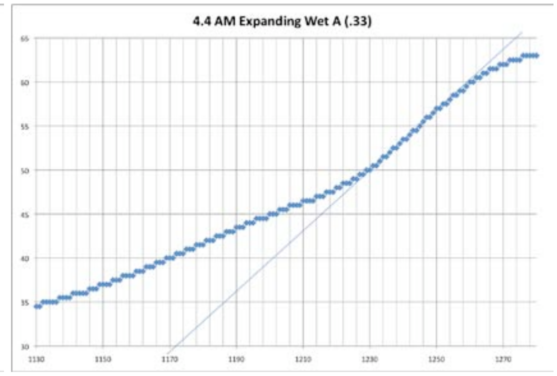
4.4 AM Expanding Wet A (.33)

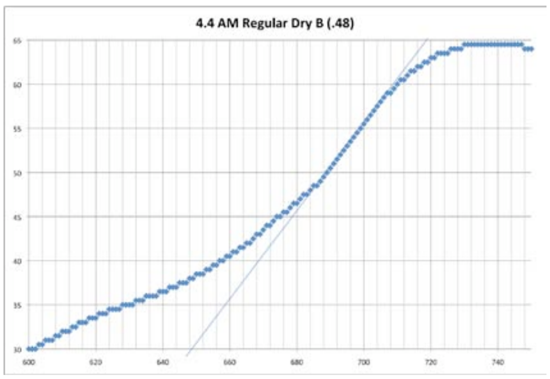
4.4 AM Regular Dry B (.48)

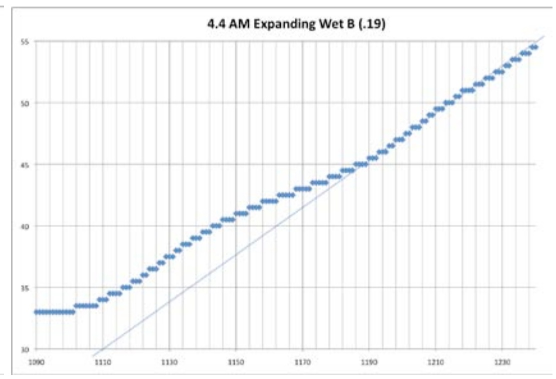
4.4 AM Expanding Wet B (.19)

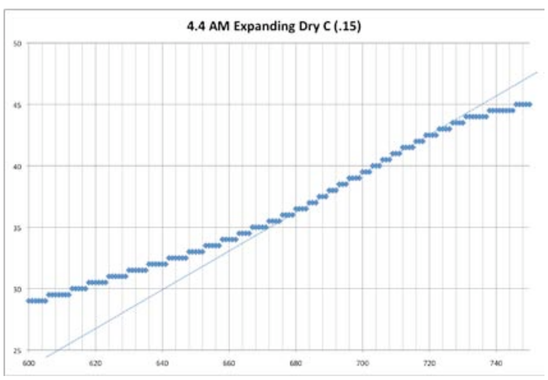
4.4 AM Expanding Dry C (.15)

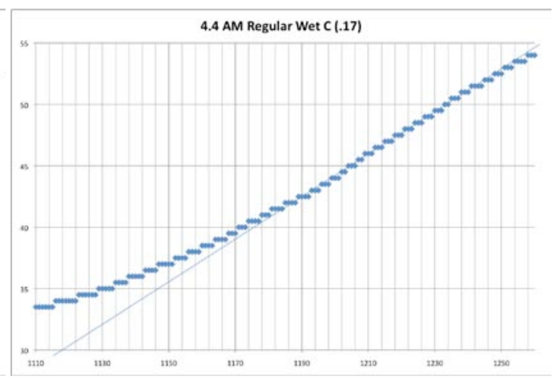
4.4 AM Regular Wet C (.17)

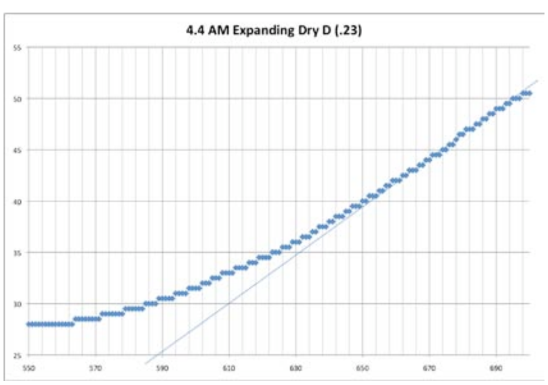
4.4 AM Expanding Dry D (.23)

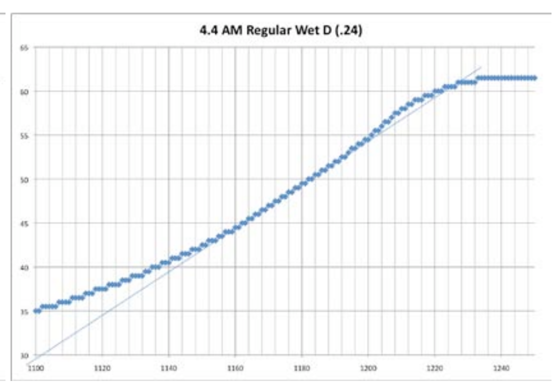
4.4 AM Regular Wet D (.24)

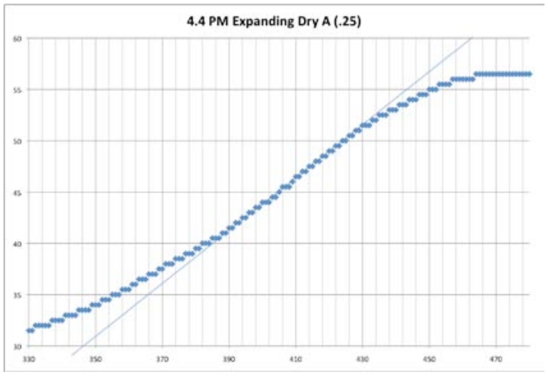
4.4 PM Expanding Dry A (.25)

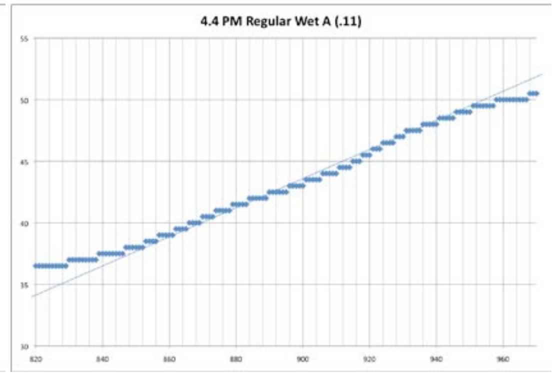
4.4 PM Regular Wet A (.11)

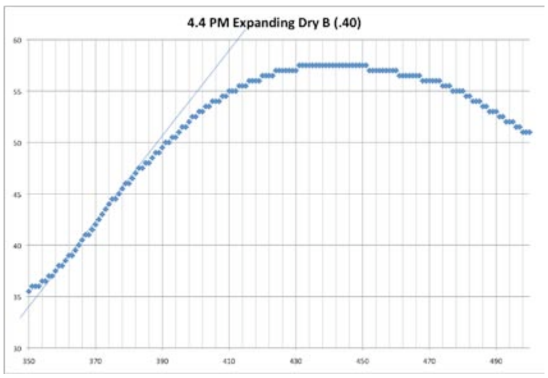
4.4 PM Expanding Dry B (.40)


4.4 PM Regular Wet B (.16)

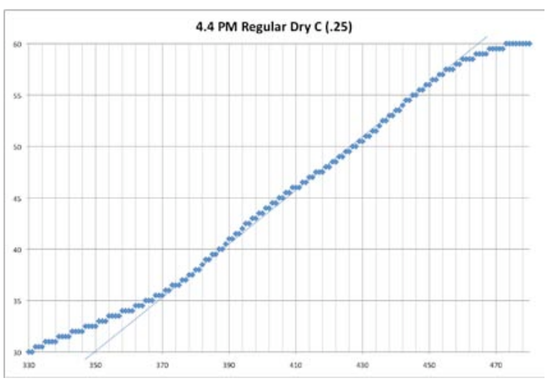
4.4 PM Regular Dry C (.25)

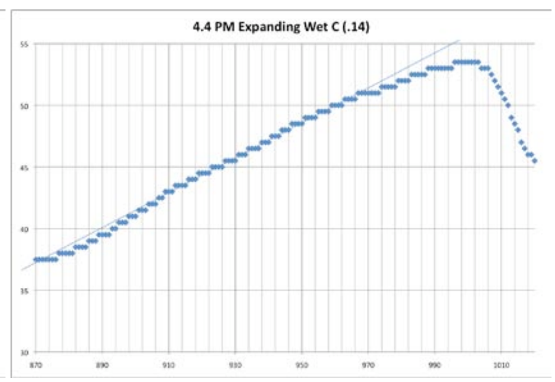
4.4 PM Expanding Wet C (.14)

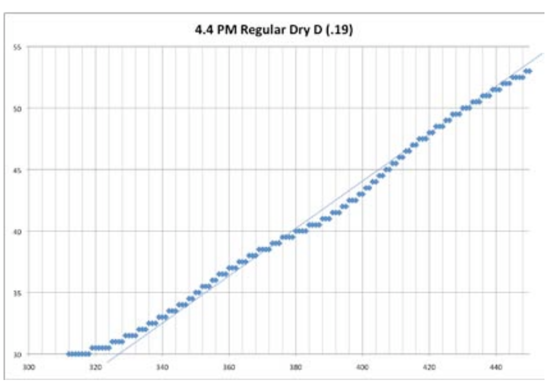
4.4 PM Regular Dry D (.19)

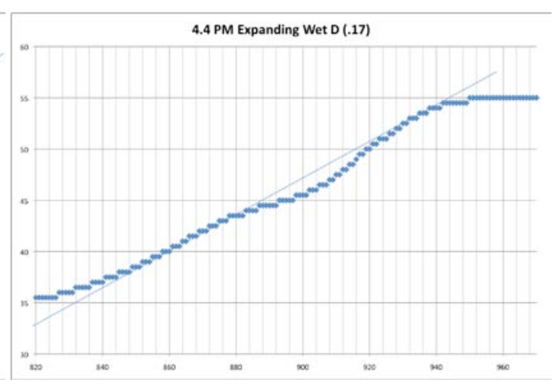
4.4 PM Expanding Wet D (.17)

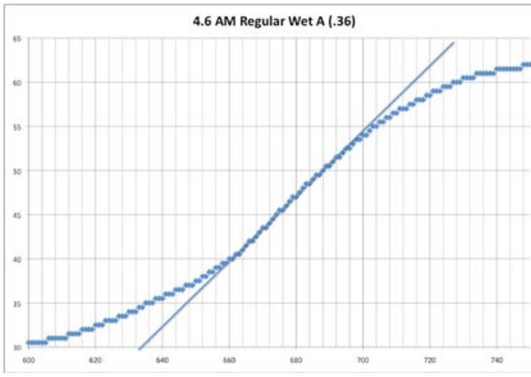
4.6 AM Regular Wet A (.36)

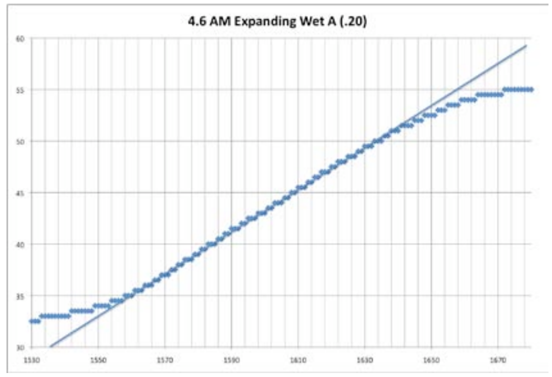
4.6 AM Expanding Wet A (.20)

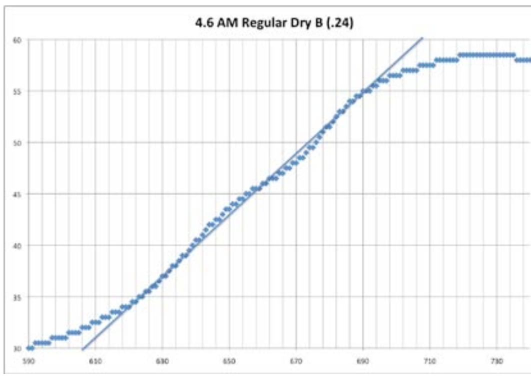
4.6 AM Regular Dry B (.24)

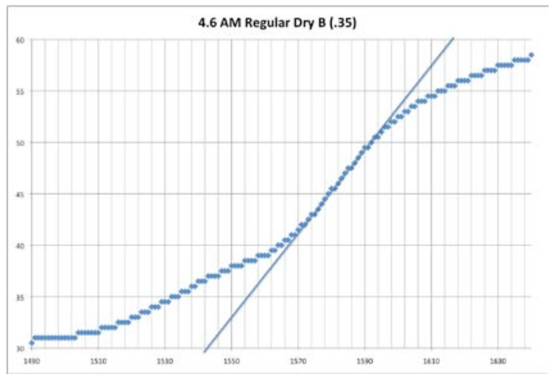
4.6 AM Regular Dry B (.35)

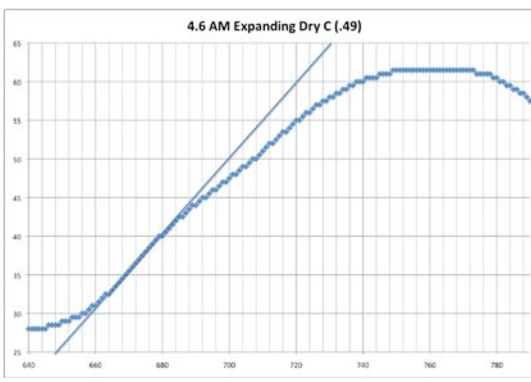
4.6 AM Expanding Dry C (.49)

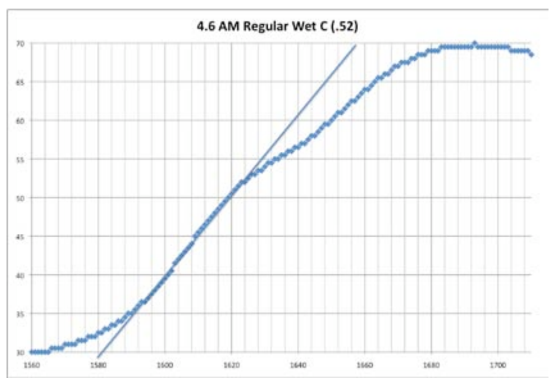
4.6 AM Regular Wet C (.52)

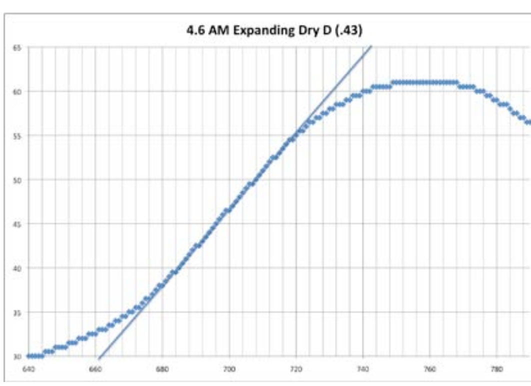
4.6 AM Expanding Dry D (.43)

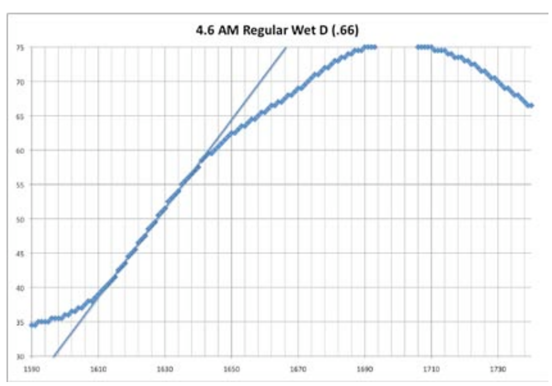
4.6 AM Regular Wet D (.66)

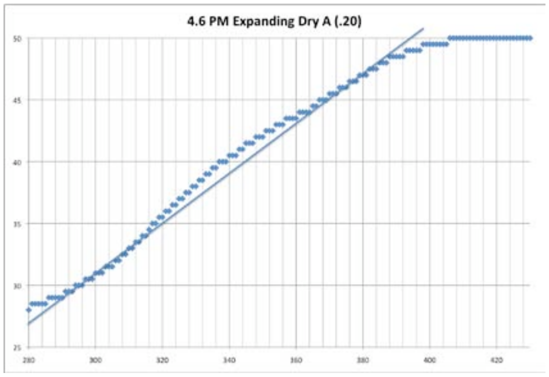
4.6 PM Expanding Dry A (.20)

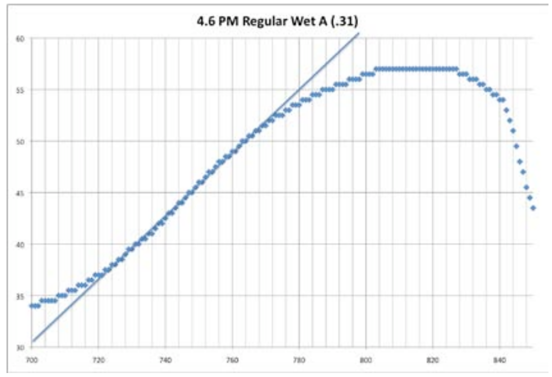
4.6 PM Regular Wet A (.31)

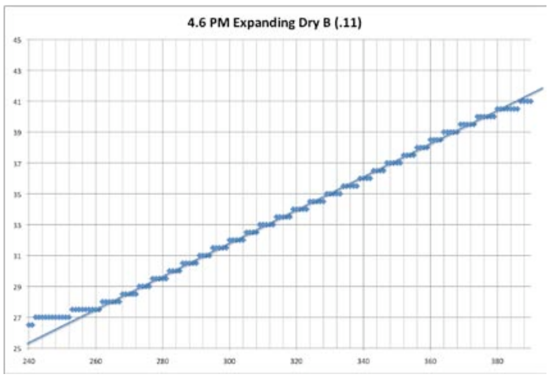
4.6 PM Expanding Dry B (.11)

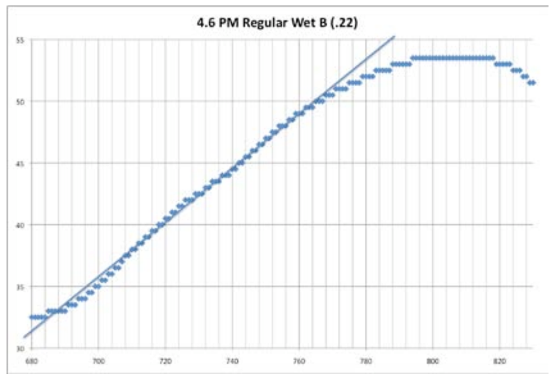
4.6 PM Regular Wet B (.22)

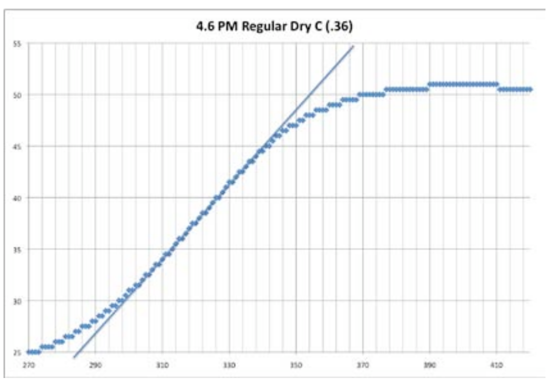
4.6 PM Regular Dry C (.36)

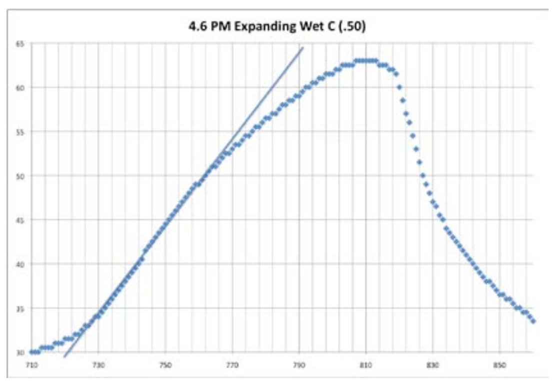
4.6 PM Expanding Wet C (.50)

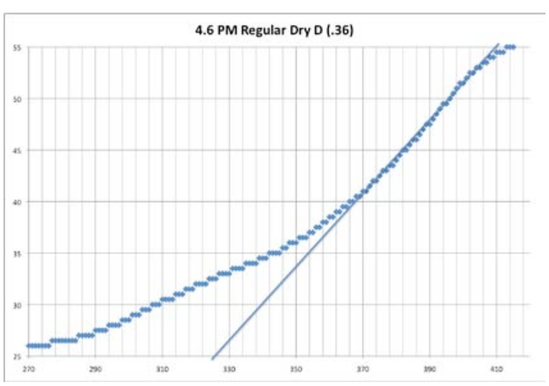
4.6 PM Regular Dry D (.36)

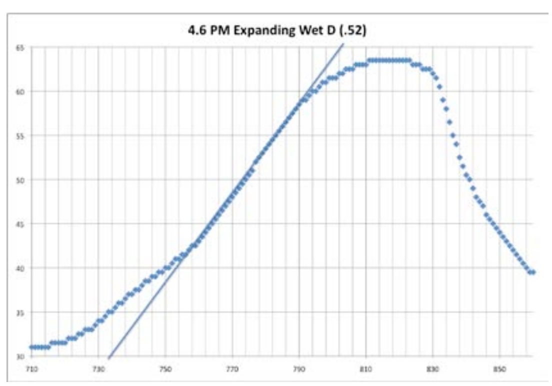
4.6 PM Expanding Wet D (.52)

Appendix B: Material Properties

These are the thermal properties of each of the layers of material employed in the present investigation. Calibrations were performed by White [17].

Material	k (W/m-K)	ρ (kg/m^3)	C_p (kJ/kg)	thickness (m)
Natural PBI	0.05	321.8	890	0.00041
Chambray	0.045	74.2	1620	0.00023
Crosstech Moisture Barrier	0.041	143.1	1900	0.000381
Glide	0.05	74.2	1620	0.00023
Cotton Shirt	0.07	316	1500	0.0015

References

[1]Hasenmeier, Paul. The History of Firefighter Personal Protective Equipment. Retrieved 6.9.2012 from <http://www.fireengineering.com/articles/2008/06/the-history-of-firefighter-personal-protective-equipment.html>

[2]Lamb, P. The Fire Helmet. Retrieved 6.9.2012 from <www.petelamb.com/helmet.htm>

[3]Lee, A. & Meyer, R. Escape Through Time. NOVA Online. Retrieved 6.9.2012 from <www.pbs.org/wgbh/nova/escape/timefire.html>

[4] NFPA. NFPA 1971: Standard on Breathing Air Quality for Emergency Services Respiratory Protection, 2008 edition. Quincy: National Fire Protection Association, 2006.

[5] "Fire and Rescue". Lion Apparel. <http://www.lionprotects.com/fire-and-rescue>, Accessed 20 May 2012.

[6] NFPA. NFPA 1989: Standard on Protective Ensembles for Structural Fire Fighting and Proximity Fire Fighting, 2007 edition. Quincy: National Fire Protection Association, 2006.

[7] Torvi, D., J. Douglas Dale, and Bernie Faulkner. Influence of Air Gaps on Bench-Top Test Results of Flame-Resistant Fabrics. Journal of Fire Protection Engineering, 10 (1) 1999.

[8] Torvi, David and Douglas Dale. Heat Transfer Model for Thin Fibrous Materials. Journal of Fire Technology, Vol. 35, No. 3, 1999.

[9] Lawson J R and Pinder T A 2000 Estimates of thermal conductivity for material used in fire fighter's protective clothing <http://fire.nist.gov/bfrlpubs/fire00/PDF/f00030.pdf> accessed 11 June 2012

[10] Stoll, A. M. and M. A. Chianta. Method and Rating System for Evaluation of Thermal Protection. Aerospace Medicine, Volume 40 (1969). p 1232-1238.

[11] Zhu, Fanglong, et al. Study of skin model and geometry effects on thermal performance of thermal protective fabrics. Heat Mass Transfer; 2008. vol. 45, pp. 99-105.

[12] Diak, Tilas and GB Delkumbeurewatte. The Influence of Moisture Content on the Thermal Conductivity of a Knitted Structure. William Lee Innovation Centre, Textile and Paper, School of Materials, the University of Manchester, Manchester, UK. Published 13 March 2007.

[13] Krasny, John, et al. Protecting Fire Fighters Exposed in Room Fires; Comparison of Results for Bench Scale Test For Thermal Protection and Conditions During Room Flashover. National Bureau of Standards, Gaithersburg, MD. Fire Technology, February 1988.

[14] Perry, Justin. "Thermal Degradation of Firefighter Turnout Gear due to the Effects of Moisture." MS thesis. University of Maryland, 2011.

[15] Hendrickson, Bryant. "The Impact of a Variable Air Gap on the Thermal Performance of Firefighter Protective Clothing." MS thesis. University of Maryland, 2011.

[16] Karlsson, Bjorn and James Quintiere. Enclosure Fire Dynamics. Boca Raton; CRC Press, 2000.

[17] White, James. "An Experimental Analysis of Firefighter Protective Clothing: The Influences of Moisture and a Thermally Activated Expanding Air-Gap." MS thesis. University of Maryland, 2012.

[18] American society for Testing Materials. ASTM D4108: Standard Test Method for Thermal Protective Performance of Materials and Clothing by Open-Flame Method (1987). West Conshohocken, PA.

[19] American Society for Testing Materials. ASTM F1939: Standard Test Method for Radiant Protective Performance of Flame Resistant Clothing Materials (1999). West Conshohocken, PA.

[20] American Society for Testing Materials. ASTM F1930: Standard Test Method for Evaluation of Flame Resistant Clothing for Protection Against Flash Fire Simulations Using an Instrumented Thermal Manikin (2000). West Conshohocken, PA.

[21] Schneider, A. M., B. N. Hoschke, and H. J. Goldsmid. "Heat Transfer Through Moist Fabrics." Textile Res J. 62.2 (1992): 61-66.

[22] “Fire and Rescue”. Lion Apparel. <http://www.lionprotects.com/fire-and-rescue>, Accessed 20 May 2012.

[23] Thermal Performance of Fire Fighter's Protective Clothing Part 1. Numerical Study of Transient Heat and Water Vapor Transfer. Prasad, K. R.; Twilley, W. H.; Lawson, J. R.

[24] K. Tanaka. "A Thermomechanical Sketch of Shape Memory Effect: One-Dimensional Tensile Behavior." Res Mechanica 18 (1986): 251-63.

[25] Chapra, S. C., and R. P. Canale. Numerical Methods for Engineers. 2nd ed. New York: McGraw-Hill, 1988.

[27] Incropera, Frank P., and David P. DeWitt. Fundamentals of Heat and Mass Transfer. New York: J. Wiley, 2002. Print.

[28] Fire-Related Firefighter Injuries in 2008. US Fire Administration, FEMA. February 2008.

[29] Spangler, K. "Energy Transport in Firefighter Protective Clothing." Thesis. University of Maryland, 2008.